

16. Pliocene-Pleistocene Variations in Aragonite Content and Planktonic Oxygen-Isotope Record in Bahamian Periplatform Ooze, Hole 633A¹

André W. Droxler,² Christopher H. Bruce,³ William W. Sager,⁴ and David H. Watkins⁵

ABSTRACT

Hole 633A was drilled in the southern part of Exuma Sound on the toe-of-slope of the southeastern part of Great Bahama Bank during ODP Leg 101. The top 55 m, collected as a suite of six approximately 9.5-m-long hydraulic piston cores, represents a Pliocene-Pleistocene sequence of periplatform carbonate ooze, a mixture of pelagic calcite (foraminifer and coccolith tests), some pelagic aragonite (pteropod tests), and bank-derived fine aragonite and magnesian calcite. A 1.6-m.y.-long hiatus was identified at 43.75 mbsf using calcareous nannofossil biostratigraphy and magnetostratigraphy.

The 43.75-m-thick periplatform sequence above the hiatus is a complete late Pliocene-Quaternary record of the past 2.15 m.y. The $\delta^{18}\text{O}$ curve, primarily based on *Globigerinoides sacculifera*, clearly displays high-frequency/low-amplitude cycles during the early Pleistocene and low-frequency/high-amplitude cycles during the middle and late Pleistocene. Variations in aragonite content in the fine fraction of the periplatform ooze show a cyclic pattern throughout the Pleistocene, as previously observed in piston cores of the upper Pleistocene. These variations correlate well with the $\delta^{18}\text{O}$ record: high aragonite corresponds to light interglacial $\delta^{18}\text{O}$ values, and vice versa. Comparison of the $\delta^{18}\text{O}$ record and the aragonite curve helps to identify 23 interglacial and glacial oxygen-isotope stages, corresponding to 10.5 aragonite cycles (labeled A to K) commonly established during the middle and late Pleistocene (0.9 Ma–present). Strictly based on the aragonite curve, another 11 aragonite cycles, labeled L to V, were identified for the early Pleistocene (0.9 to 1.6 Ma). Mismatches between the $\delta^{18}\text{O}$ record and the aragonite curve occur mainly at some of the glacial-to-interglacial transitions, where aragonite increases usually lag behind $\delta^{18}\text{O}$ depletion. When one visually connects the minima on the Pleistocene aragonite curve, low-frequency (0.4 to 0.5 m.y.) supercycles seem to be superimposed on the high-frequency cycles. The timing of this supercycle roughly matches the timing of the Pleistocene carbonate preservation supercycles described in the Pacific, Indian, and Atlantic oceans. Mismatches between aragonite and $\delta^{18}\text{O}$ cycles are even more obvious for the late Pliocene (1.6 to 2.15 Ma). Irregular aragonite variations are observed for the late Pliocene, although after the onset of late Pleistocene-like glaciations in the North Atlantic Ocean 2.4 m.y. ago the $\delta^{18}\text{O}$ record has shown a mode of high-frequency/low-amplitude cycles. Initiation of climatically induced aragonite cycles occurs only at the Pliocene-Pleistocene transition, 1.6 m.y. ago. After that time, aragonite cycles are fully developed throughout the Quaternary.

The 11-m-thick periplatform sequence below the hiatus represents a lower Pliocene interval between 3.75 and 4.45 Ma. The bottom half (4.25–4.45 Ma) has a fairly constant, high aragonite content (averaging 60%) and high sedimentation rates (28 m/m.y.) and corresponds to the end of the prolonged early Pliocene interglacial interval (4.1–5.0 Ma), established as a worldwide high sea-level stand. The second half (3.75–4.25 Ma), in which aragonite content decreases by successive steps, paralleled by a gradual $\delta^{18}\text{O}$ enrichment in *Globigerinoides sacculifera* and low sedimentation rates (10 m/m.y.), corresponds to the climatic deterioration established worldwide between 4.1 and 3.8 Ma, to a decrease of carbonate preservation observed in the equatorial Pacific Ocean, and to a global sea-level decline. Dolomite, a ubiquitous secondary component in the lower Pliocene, is interpreted as being authigenic and possibly related to diagenetic transformation of primary bank-derived fine magnesian calcite.

Transformation of the primary mineralogical composition of the periplatform ooze was evidently minor, as the sediments have retained a detailed record of the Pliocene-Pleistocene climatic evolution. Clear evidence of diagenetic transformations in the periplatform ooze includes (1) the disappearance of magnesian calcite in the upper 20 m of Hole 633A, (2) the occurrence of calcite overgrowths on foraminiferal tests and microclasts at intermittent chalky core levels, and (3) the ubiquitous presence of authigenic dolomite in the lower Pliocene.

INTRODUCTION

Periplatform ooze separating turbidite layers of lime mud or sand and deposited in the vicinity of shallow carbonate banks is a mixture of pelagic ooze (coccoliths and foraminifers composed of calcite [less than 4 mol% MgCO_3] and pteropods composed of aragonite) and a variable proportion of bank-derived

fine aragonite and magnesian calcite (more than 4 mol% MgCO_3) (Schlager and James, 1978). Sea-level fluctuations, which, to a great extent, influence the sediment production and export from the shallow banks, are preserved in the mineral composition of the periplatform ooze owing to the different carbonate mineralogy of pelagic and bank-derived components. Because aragonite and magnesian calcite are metastable relative to calcite, their degree of preservation or removal by dissolution at the seafloor is related to variations of the carbonate saturation state within the overlying water masses, and this may overprint the primary mineralogical input signal. Furthermore, the admixture of the metastable carbonate phases (aragonite and magnesian calcite) relative to pure pelagic calcite gives periplatform ooze a greater diagenetic potential than pure pelagic calcitic ooze.

In the Bahamas, upper Quaternary periplatform ooze shows cyclic variations of aragonite content in the fine fraction (<62 μm), in addition to cyclic variations of total carbonate and quartz

¹ Austin, J. A., Jr., Schlager, W., et al., 1988. *Proc. ODP, Sci. Results*, 101: College Station, TX (Ocean Drilling Program).

² Department of Geology and Geophysics, Rice University, P.O. Box 1892, Houston, TX 77251.

³ Department of Geology, Oxygen Isotope Laboratory, University of South Carolina, Columbia, SC 29208.

⁴ Department of Oceanography, Texas A&M University, College Station, TX 77843.

⁵ Department of Geology, University of Nebraska, 330 Bessey Hall, Lincoln, NE 68588-0340.

content (Supko, 1963; Kier and Pilkey, 1971; Droxler et al., 1983; Boardman et al., 1986; Slowey, 1985). This is also true on the Nicaraguan Rise (Caribbean Sea) and in the Maldives (Indian Ocean) (Droxler, 1986a). Aragonite cycles, as well as carbonate-terrigenous cycles, are closely correlated with the oxygen-isotope record of planktonic foraminifers (Droxler et al., 1983; Boardman et al., 1986; Droxler, 1986a) and thus may be climatically induced cycles corresponding to the long series of glacial-interglacial alternations observed since the onset of major glaciation in the North Atlantic Ocean 2.4 m.y. ago (e.g., Shackleton et al., 1984). Although the relationship between climatic variations and aragonite cycles in periplatform ooze is clear during the late Quaternary, the real causes of these aragonite cycles are still a subject of controversy (see Droxler and Schlager, 1985b; Droxler, 1986b; Boardman and Neumann, 1985, 1986). We have interpreted aragonite cycles as a dissolution-preservation imprint on an input signal of bank-derived aragonite related to the flooding and exposure of the shallow banks. According to this interpretation, aragonite cycles in intermediate water masses would be analogous to the glacial carbonate dissolution cycles of the deep Atlantic. Another group of researchers, led by Boardman and Neumann, argues that the aragonite cycles are a pure input signal of bank-derived aragonite related to the flooding and exposure of the shallow banks, and therefore a detailed sea-level indicator.

Coring in the Bahamas during Leg 101 of the Ocean Drilling Program recovered thick undisturbed sequences of periplatform ooze with the hydraulic piston corer (HPC). This was a unique opportunity to extend the available 12- to 18-m penetrations of this ooze by regular piston coring (corresponding in age to late or middle Pleistocene). By recovering thicker periplatform sequences, three new questions could be addressed: (1) How did the climatically induced aragonite cycles, well-established during middle to late Pleistocene, evolve during the early Pleistocene and the Pliocene? How do they record major climatic events (e.g., the onset of major glaciations around the North Atlantic Ocean at 2.4 Ma)? (2) How well does the aragonite content in the fine fraction correlate with the oxygen-isotope record on planktonic foraminifers for the entire Pliocene-Pleistocene? (3) How much has the primary depositional record been modified by early burial diagenesis, owing to the presence of metastable aragonite and magnesian calcite components in the periplatform ooze? In this regard, some research in the Bahamas has predicted that aragonitic components would be rapidly replaced by more stable carbonate phases such as calcite and perhaps dolomite.

SITE LOCATION AND DESCRIPTION

Hole 633A was drilled in the southern part of Exuma Sound on the toe-of-slope of the Great Bahama Bank, in 1681 m water depth (Fig. 1). Only the top 55 m of Hole 633A was studied in this research program. This interval corresponds almost exclusively to lithologic Unit I, defined in Austin, Schlager, et al. (1986) as a periplatform-ooze sequence with cyclic variations in color and a few scattered 1- to 10-cm-thick calcareous turbidite layers. Considering the proximal position of Hole 633A, the fine-grained turbidites in Unit I are unusually thin. These characteristics can be explained by the location of the site on a topographic high that rises 20 to 40 m above the surrounding seafloor and could be caused by progradation of a spur of the gullied slope or by large-scale slumping prior to the deposition of Unit I (Austin, Schlager, et al., 1986).

METHODS

Sediment Sampling and Analyses

The top 55 m of Hole 633A was sampled every 10 cm; care was taken to avoid sampling turbidite layers and zones with obvious reworking or

disturbed features. Each 10-cm³ sediment sample was dried in an oven at 60°C, weighed, and suspended in distilled water (pH 8). The coarse fraction of the sediment was separated from the fine fraction through a 62- μ m-mesh sieve and then dried at 60°C and weighed again. The fine fraction (less than 62 μ m) was left to stand in distilled water for a day or two until the particles were completely settled, and was then dried at 60°C. The coarse fraction was used to establish the Menardii Complex stratigraphy, to estimate the degrees of cementation and overgrowth, and to pick monospecific samples of planktonic foraminifers—*Globigerinoides sacculifera* and *Globigerinoides rubra* (pink)—for oxygen-isotope analyses. The fine fraction was used for carbonate-mineralogy analyses by X-ray diffraction and for carbonate-content analyses by carbonate bomb. Bulk samples at 0.5-m intervals were used to establish the calcareous nannofossil biostratigraphy by smear slide and SEM analyses, and oriented samples were taken at 0.5- to 1-m intervals to develop magnetostratigraphy; analyses were conducted on a cryogenic magnetometer made available to us at the University of Texas at Austin.

Carbonate Content in Fine Fraction (<62 μ m)

The carbonate-bomb method was used to determine the total carbonate content of the fine fraction in each sample from the CO₂ pressure generated by dissolving the carbonate fraction in 50% concentrated HCl (Müller and Gastner, 1971). The pressure of CO₂ released by the fraction of the carbonate with the acid was compared with pressure released by an equal amount of 100% CaCO₃ standard. Accuracy of the method for marine sediments remained within $\pm 2\%$ for CaCO₃ values ranging between 5% and 95% (Birch, 1979).

Carbonate Mineralogy (<62 μ m)

Relative proportions of the different carbonate minerals were quantified by X-ray-diffraction analyses. Each sample of fine sediment was dried at 60°C, ground for less than a minute by hand in an agate mortar, sieved to obtain an agglomerate of <62 μ m particles, and packed with a spatula into an aluminum sample holder. The effects of particle size and grinding are minimized through these procedures (Milliman, 1974). Each sample was then analyzed using a Norelco-Philips X-ray diffractometer at 30 KV and 20 Ma, through a scan from 32° to 25°, at low scanning speed of 0.25°/minute for optimal resolution. Areas under the aragonite peak, the dolomite peak (if present), the calcite peaks (calcite and magnesian calcite = total calcite), and under the half lower 2 θ angles of the calcite peak (since calcite was always larger than magnesian calcite) were measured by planimeter. The calcite area was calculated by doubling its measured half-peak area and the magnesian calcite area by subtracting the area of calcite from the measured area under the total calcite peaks. The aragonite portion in each sample was calculated with an accuracy of better than 5% from a calibration curve (Droxler, 1984). Reproducibility of the method used to separate calcite from magnesian calcite is within a measured maximum discrepancy of 9%. Because of the linear relationship between dolomite and calcite (Milliman, 1974, p. 26), the dolomite proportion was calculated by a ratio of the dolomite-peak area and the total area of both dolomite and total calcite peaks.

Stratigraphy

Calcareous-Nannofossil Biostratigraphy. Nannofossil assemblages were examined using light microscopy on smear slides of raw sediment and on gravitationally concentrated samples. Biostratigraphic age determinations were based on first- and last-occurrence datums using the geochronologic assignments of Berggren et al. (1985). In general, nannofossil abundances in the smear slides of raw sediment varied from approximately 70% to less than 5%, with platform-derived debris composing much of the rest of the sample. Samples from Hole 633A exhibited a notable covariance of nannofossil preservation and abundance. Preservation was excellent in Quaternary nannofossil oozes, which contained little or no significant platform-derived components. The original forms of the taxa were retained, with infilling of the central area only rarely occurring in taxa such as *gephyrocapsids*. Poorer preservation was typical of Quaternary and Pliocene periplatform oozes, with 24%–40% nannofossils in the smear slides. Overgrowths were the most common diagenetic alteration of larger nannofossils in these samples. Etching of smaller coccoliths was common. Samples with less than 10% nannofossil material tended to be very poorly preserved. Overgrowth of discoasters and large placoliths was intense in these samples, commonly obscuring taxonomic affinities. Most of the more delicate taxa have been destroyed by dissolution.

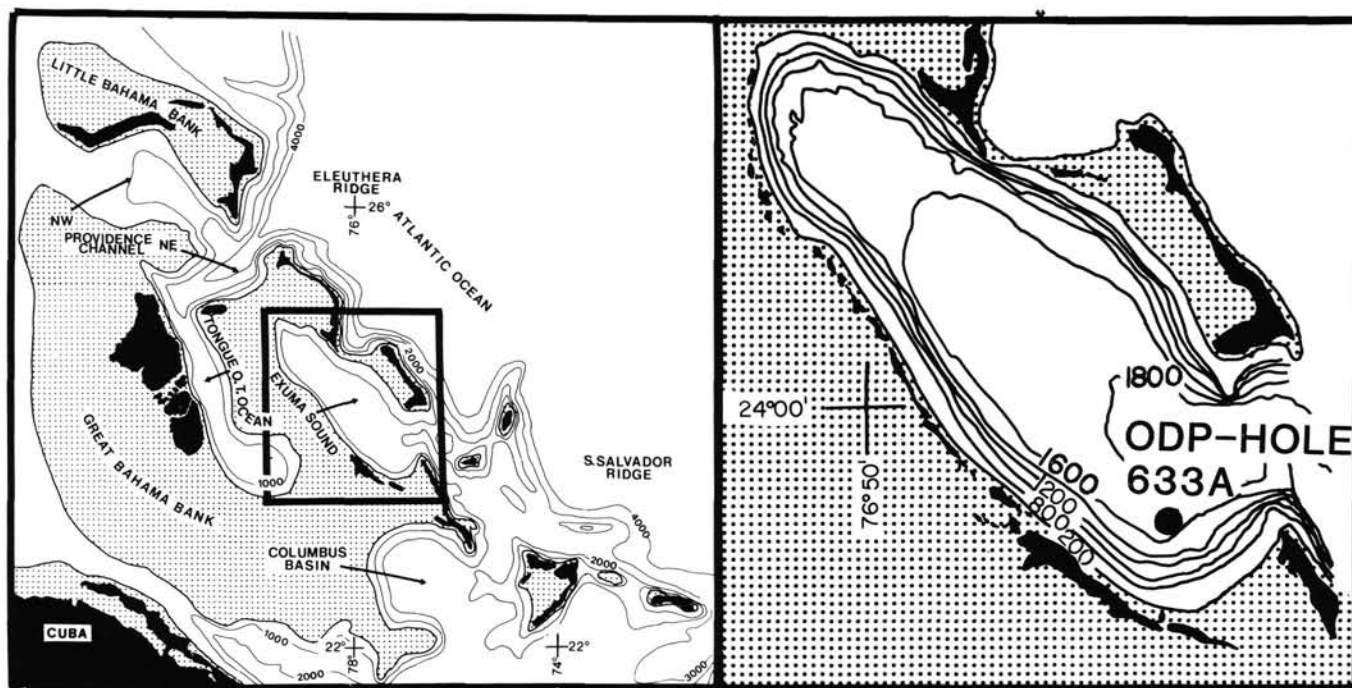


Figure 1. Location maps, Hole 633A. Contours (in meters) after King (1969); insert modified from Crevello and Schlager (1980). Dotted pattern delineates carbonate banks shallower than 20 m.

Globorotalia menardii Complex. The *Globorotalia menardii* Complex, referred to later in this discussion as Menardii Complex, was established by observing the $> 300 \mu\text{m}$ size fraction to determine presence or absence of the three subspecies of the Menardii Complex: *Globorotalia menardii*, *Globorotalia menardii tumida*, *Globorotalia menardii flexuosa*. The different zones of the Menardii Complex stratigraphy (defined by Ericson and Wollin, 1966) were identified in Hole 633A from zone Z down to possibly zone P.

Magnetostratigraphy. Magnetic characteristics of 102 oriented samples from Hole 633A were measured with an SCT cryogenic magnetometer. The NRM intensities of these samples varied systematically through more than two orders of magnitude. Samples in the upper 30 m of Hole 633A were the most strongly magnetic, having NRM intensities as high as 9×10^{-3} A/m. In the rest of the hole, the NRM intensities averaged 5×10^{-5} A/m. Stable remanent magnetic directions were determined by stepwise alternating-field demagnetization. Because many of the samples were relatively weakly magnetic, each value of the remanent direction was determined by averaging at least six individual measurements. In this manner, random scatter from thermal and electrical noise in the magnetometer was reduced. An interpretation of magnetic polarity was made for each sample using its stable magnetic inclination. Normally polarized samples yielded inclinations in the average of 44° downward (the geocentric axial dipole inclination for Hole 633A), whereas reversely polarized samples showed inclinations of about 44° upward.

Oxygen Isotopes

Oxygen isotopes were analyzed on hand-picked samples of *Globigerinoides sacculifera* down to Section 633A-6H-1 (47 m sub-bottom), and of *Globigerinoides rubra* (pink) occasionally in the upper 7 m of Hole 633A, using the same 10-cm spaced sample whose fine fraction was used for mineralogical studies. For each sample, 10 to 20 foraminifer tests were picked in a narrow size fraction between 300 and 350 μm , cleaned ultrasonically to remove any calcareous mud clinging to the tests, dried at 60°C , and roasted at $370^\circ\text{--}380^\circ\text{C}$ for 1 hr under vacuum. They were then reacted at 60°C with excess 100% H_3PO_4 , and the CO_2 gas was analyzed in one of the two mass spectrometers (VG SIRA 24 and VG Micromass 602) at the Stable Isotope Laboratory of the University of South Carolina. Results are reported relative to the PDB standard. Analytical precision on standards and duplicated samples was 0.15‰ and 0.25‰, respectively.

RESULTS

Establishment of a Pliocene Hiatus

Calcareous-Nannofossil Biostratigraphy

Examination of the top 55 m of Hole 633A for calcareous-nannofossil biostratigraphy shows that the Quaternary and upper Pliocene are quite complete through the *Calcidiscus macintyre* Subzone (CN12d) down to 43.75 m (Section 101-633A-5H-5), where the CN12d Subzone lies directly on the *Amaurolithus tricorniculatus* Zone (CN10). The hiatus includes Subzones CN11 to CN12c and may also include the upper part of CN10 as well (CN10c?). The generally poor preservation of the nannofossil assemblage in this part of Core 101-633A-6H makes it difficult to determine exactly how much of uppermost Zone CN10 is missing. Figure 2 shows the timing of the nannostratigraphy of the Quaternary-Pliocene interval according to Berggren et al. (1985). The age of the sediment just below the hiatus is not well constrained and could range between 3.8 and 4.4 Ma. On the other hand, sediment age just above the hiatus can be estimated to be confined between 2.1 and 2.2 Ma., because a 0.3-m.y.-long CN12d Subzone is only partially represented. The Pliocene hiatus therefore represents a time interval as long as 1.7 to 2.3 m.y.

Figure 3 shows an age vs. depth curve based on the coccolith subzones for Hole 633A. The Quaternary is defined by the beginning of the *Gephyrocapsa caribbeanica* Subzone (CN13b) at 1.6 m.y. The average sedimentation rate of 23 m/m.y. does not display any noticeable break at that time boundary. During the late Pliocene, the average sedimentation rate dropped to 12 m/m.y., about half that of the Quaternary. Below the hiatus, the sedimentation rate in Core 101-633A-6H is difficult to estimate, because its sediment is within a single coccolith zone (*Amaurolithus tricorniculatus* Zone.) However, by extrapolation with the biostratigraphy of older sediment in Core 101-633A-7H, the sedimentation rate can be roughly estimated as 28 m/m.y.

Magneto-Stratigraphy	Epochs		Age m.a.	Calcareous Nannofossil Biostratigraphy			Age of Boundary	HOLE-633A		
	Holocene			ZONES	SUBZONES					
Brunhes	Pleistocene	late	1	CN15	<i>Emiliana huxleyi</i>	ACME CN15	E. huxleyi	-0.08 (m.a.)	? Hiatus ?	
		mid.		CN14	<i>Gephyrocapsa oceanica</i>	CN14b	<i>Gephyrocapsa oceanica</i>			-0.26
early	2	CN13	<i>Crenalithus doronicoides</i>			CN14a	<i>Pseudoemiliana lacunosa</i>			-0.45
				CN13b	<i>Gephyro. caribbeanica</i>		-0.90			
Matuyama	Pliocene	late	3	CN12	<i>Discoaster brouweri</i>	CN13a	<i>Emiliana annula</i>	-1.60		
						CN12d	<i>Calcidiscus macintyreii</i>	-1.90		
						CN12c	<i>Disco. pentaradiatus</i>	-2.20		
Gauss	Pliocene	late	3	CN12	<i>Discoaster brouweri</i>	CN12b	<i>Disco. sulculus</i>	-2.40		
						CN12a	<i>Disco. tamalis</i>	-2.60		
Gilbert	Pliocene	Early	4	CN11	<i>Reticulofenestra pseudoumbilica</i>	CN11b	<i>Disco. asymmetricus</i>	-3.40		
						CN11a	<i>Sphenolithus neobabies</i>	-3.60		
						CN10	<i>Amaurolithus tricorniculatus</i>	CN10c	<i>Ceratolithus rugosus</i>	-3.70
								CN10b	<i>Ceratolithus acutus</i>	-4.50
5				-5.00						

Figure 2. Top 70 m of Hole 633A placed on a time scale based on general calcareous-nannofossil biostratigraphy (from Berggren et al., 1985) and on general magnetostratigraphy (from Harland et al., 1982). Minimum and maximum possible extension of Pliocene hiatus in Hole 633A is also shown.

Magnetostratigraphy

The hiatus at 43.75 mbsf, well defined by biostratigraphy, is recorded by the absence of the Gauss normal Chron in the variations through time of the paleomagnetic inclinations (Fig. 4). Above the hiatus are the Brunhes and Matuyama Chrons, and the switch from normal to reverse inclination is at 16.75 mbsf. Jaramillo, Olduvai, and possibly Reunion normal events are observed within the Matuyama reversed Chron. The earliest 0.2 m.y. of the Matuyama Chron seems to be missing. Below the hiatus, the four normal events within the Gilbert reversed Chron (Cochiti, Nunivak, and Sidufjall, as well as the top of the Thvera) are observed.

By plotting the age of the successive boundaries of the paleomagnetic events (Harland et al., 1982) on an age vs. depth curve (Fig. 4), downcore variations of sedimentation rate can be calculated, and the timing of the hiatus can be better constrained. Above the hiatus, sedimentation rate increases by a factor of 2 at around 1.65 Ma, in support of the age vs. depth curve based on calcareous-nannofossil biostratigraphy (Fig. 3). By extrapolating the calculated sedimentation rate of 11 to 12 m/m.y. between 1.6 and 2.2 Ma, the age of the sediment just above the hiatus is estimated to be 2.15 Ma. The occurrence of the four events within the Gilbert Chron helps in calculating the variation of sedimentation rate during the early Pliocene. This could not be done using nannofossil biostratigraphy because of low resolution owing to the poor preservation of the material. The highest sedimentation rate during the Pliocene-Pleistocene (28 m/m.y.) was recorded during the period before 4.25 Ma. It drops by a factor of almost 3 to 10 m/m.y. between 4.25 and 3.9 Ma. By extrapolation of this low sedimentation rate, the age of the sediment just below the hiatus was estimated to be 3.75 Ma. Therefore, based in part on the nannofossil biostratigraphy but mainly on the magnetostratigraphy, the upper Pliocene hiatus corresponds to a time interval of approximately 1.6 m.y., and the upper 55 m of Hole 633A can be subdivided into four time

intervals: (1) Holocene through upper to middle Pleistocene 0.00–0.90 Ma, 00.00–20.50 mbsf; (2) lower Pleistocene, 0.90–1.60 Ma, 20.50–36.50 mbsf; (3) upper Pliocene, 1.60–2.15 Ma, 36.50–43.75 mbsf; and (4) lower Pliocene, 3.75–4.40 Ma, 43.75–55 mbsf.

Pliocene–Pleistocene Variations in Lithology, Carbonate Content, Carbonate Mineralogy, and Quartz Occurrence

Results from analyses of lithology, carbonate content, carbonate mineralogy, and quartz occurrence are organized in the four time intervals defined by nannofossil biostratigraphy and magnetostratigraphy (see previous section).

Holocene Through Upper to Middle Pleistocene (Fig. 5)

The top 20.5 m of Hole 633A corresponds to the past 0.9 to 1.0 m.y. The timing of this interval is well constrained by nannofossil biostratigraphy, by the Menardii Complex zones, and by magnetostratigraphy. Several nannofossil zones occur in that interval. The acme zone of *Emiliana huxleyi* is present in the top 2 m, therefore making it younger than 0.085 Ma and the beginning of *Emiliana huxleyi* at 6.20 mbsf dated as 0.25 Ma (Thierstein et al., 1977). The end and beginning of the *Pseudoemiliana lacunosa* Subzone, close in age to 0.45 Ma and 0.9 Ma, respectively (Berggren et al., 1985), occur at 9.00 mbsf and 21.5 mbsf. None of the intermediate subzones is missing. The expected Menardii Complex zones, from Z (0–0.3 mbsf, corresponding to the Holocene) to T, are present. The boundary between the Brunhes/Matuyama Chron, dated at 0.73 Ma, occurs at 16.75 mbsf. The Jaramillo normal event (between 0.92 and 0.97 Ma) occurs close to 20 mbsf. Overall, this sediment is a periplatform ooze with less than 1% chalk, observed only rarely in the vicinity of turbidite layers.

Carbonate content of the fine fraction varies between 82% and 96% and shows irregular fluctuations with minima averag-

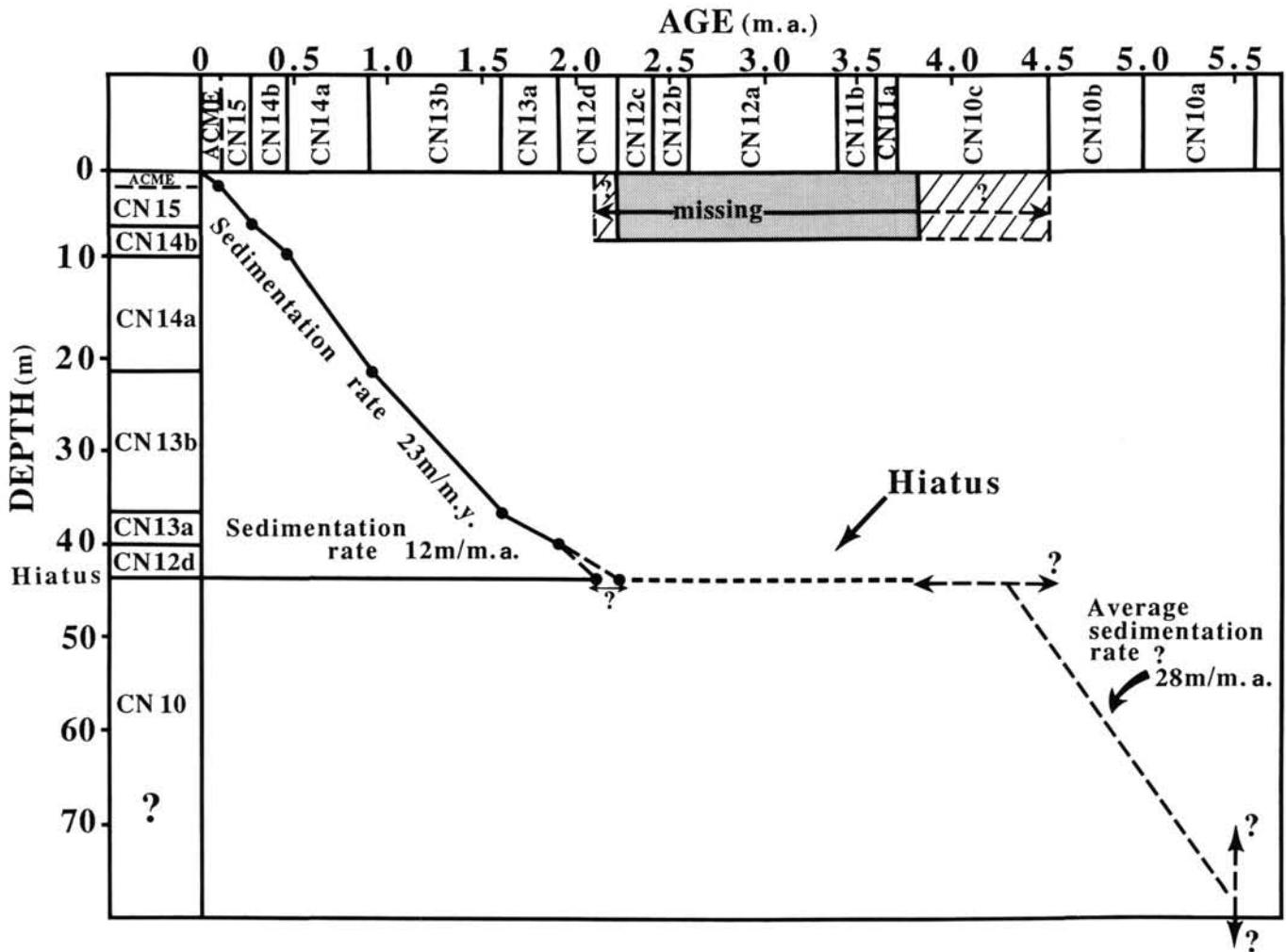


Figure 3. Age vs. depth curve for top 65 m of Hole 633A based on calcareous-nannofossil stratigraphy (from Berggren et al., 1985). Note the break in sedimentation rates by a factor of 2 at 1.6 Ma, from 23 m/m.y. to 12 m/m.y., the general Pliocene hiatus between 2.2 (2.1) Ma and 3.75 (4.4) Ma. The sedimentation rate below the hiatus is only a rough average estimate (28 m/m.y.).

ing 87% and maxima around 95%. The lowest values of carbonate content (e.g., 82% at 10.25 mbsf) correspond to clay-rich layers that were observed in the middle Pleistocene section at some of the other Leg 101 sites north of Little Bahama Bank and in Exuma Sound as well as in one piston core from the Northwest Providence Channel (Slowey, 1985). Quartz, as expected, is always related to low-carbonate intervals.

The suite of carbonate minerals includes aragonite, calcite, magnesian calcite, and dolomite in the Holocene and the upper and middle Pleistocene. Aragonite and calcite are the two major components; magnesian calcite and dolomite are secondary minerals. Aragonite maxima fluctuate between 50% and 80%, and aragonite minima between 5% and 40%. Magnesian calcite reaches a maximum value of 15% at the top of Hole 633A and gradually decreases downcore. It disappears at 6 mbsf and reappears only twice, in the two most aragonite-rich intervals (between 12.5–14 mbsf and 17.75–19.80 mbsf). Traces of dolomite appear only with the clay-rich layers and could be either detrital or diagenetic (formed by magnesium release of some of the clays).

As previously observed in piston cores (Droxler et al., 1983; Boardman et al., 1986; Slowey, 1985), aragonite content displays a regular cyclic pattern. Each cycle has an asymmetric shape representing a sharp aragonite increase followed by a more

gradual decrease. These cycles have been correlated with the oxygen-isotope record from planktonic foraminifers for the past 0.35 to 0.5 m.y. (Droxler et al., 1983; Boardman et al., 1986) and are therefore interpreted as climatically induced glacial/interglacial cycles. High values of aragonite and carbonate content correspond to light $\delta^{18}\text{O}$ and thus interglacial intervals, whereas low values of aragonite and carbonate content correspond to heavy $\delta^{18}\text{O}$ and thus glacial intervals. In the past 0.9 to 1 m.y., 10.5 aragonite cycles can be distinguished. They are labeled from A through K, starting at the top of Hole 633A, as defined in Droxler et al. (1983). Each cycle starts with the sharp aragonite increase characteristic of the glacial/interglacial transition and includes an interglacial interval and the following glacial interval. Cycle A, corresponding to the Holocene, is therefore only a half cycle. A similar continuous Holocene through upper to middle Pleistocene aragonite record was described by Slowey (1985) in a 17.5-m-long piston core from Northwest Providence Channel. The overall pattern of aragonite cycles in this piston core correlates well with those displayed in the top 21 m of Hole 633A.

The coarse fraction usually makes up less than 20% of the total sediment, and only partial overgrowths on the foraminifer tests are observable in some of the lowest aragonite glacial intervals, such as in cycles D, F, and K. The average rate of sedimen-

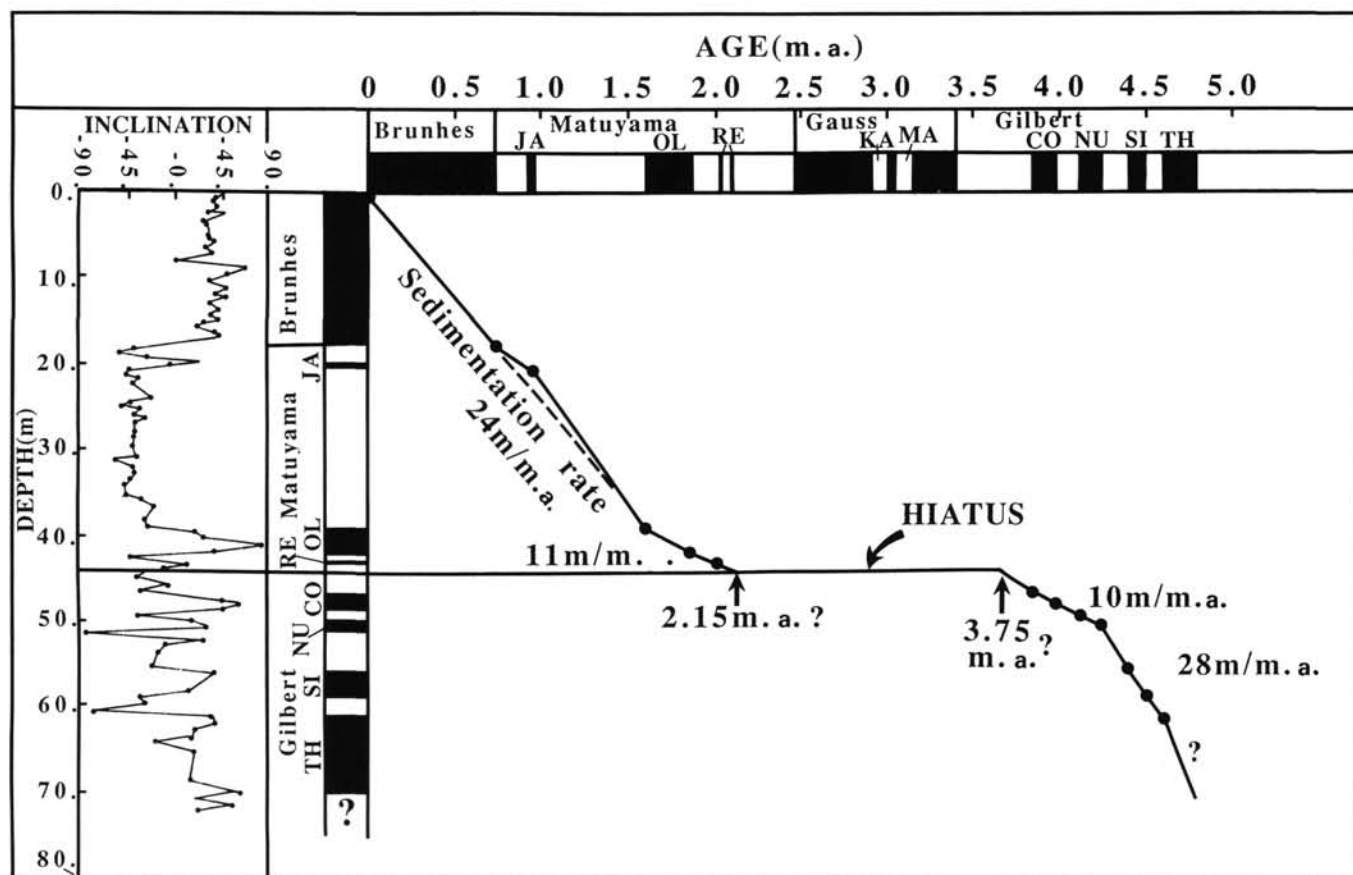


Figure 4. Age vs. depth curve for top 70 m of Hole 633A based on magnetostratigraphy (Harland et al., 1982). Note the good agreement above Pliocene hiatus with Figure 3. The presence of several normal events during the Gilbert Chron helps to bring out a break in sedimentation rate by a factor of almost 3 at ~50 mbsf from 10 m/m.y. to 28 m/m.y. Hiatus is constrained in age between 2.15 and 3.75 Ma by extrapolating sediment rates just above and below hiatus.

tation (23 to 24 m/m.y.) during the late to middle Pleistocene is identical to that estimated for the early Pleistocene.

Lower Pleistocene (Fig. 6)

The lower Pleistocene sequence is constrained within the single nannofossil subzone *Gephyrocapsa caribbeanica* (CN13b) and the S and R zones of the Menardii Complex. It represents the reverse Matuyama Chron, devoid of any normal events between the Jaramillo and Olduvai, and can be dated fairly accurately between 0.9 and 1.6 Ma. This time interval has the most turbidite layers of the Pliocene-Pleistocene sequence in Hole 633A. However, these turbidites, some several tens of centimeters thick, constitute no more than 15% of the total sediment. Less than 10% of the periplatform ooze is sufficiently indurated to be considered chalk.

Carbonate content in the fine fraction fluctuates between 80% and 90%. The largest fluctuations occur in the bottom half of Sections 101-633A-4H-4 through 101-633A-4H-6, corresponding approximately to a time interval between 1.3 to 1.6 Ma. For this time, spikes of low carbonate values correspond to short events (usually within a 10-cm-thick interval). Between 0.9 and 1.3 m.y. (21 to 32 mbsf), the carbonate values remain above 90%, averaging 94%. Quartz-rich intervals correlate with the lowest carbonate values and are generally thinner than similar intervals in the upper Pliocene or the upper to middle Pleistocene.

Aragonite and calcite are the two carbonate phases in the fine fraction. Aragonite content varies from 10% to 80% and displays well-defined asymmetric cycles with a sharp increase followed by a gradual decrease, especially between 0.9 and 1.3 Ma. At the bottom of the lower Pleistocene, these aragonite cycles become more irregular. Eleven aragonite cycles (labeled L through V in Fig. 6), as defined in the previous section, can be counted during the 0.7-m.y.-long record of this lower Pleistocene section. High aragonite intervals do not always correspond to the highest carbonate values, especially at the bottom of the lower Pleistocene, where the short-term carbonate minima usually occur during the sharp transition from low to high aragonite content or at the aragonite maxima.

The coarse fraction usually makes up less than 20% of the total sediment. Larger values (20% to 60%) occur only during low-aragonite intervals, where some cementation is observed in the form of overgrowths on foraminifer tests and microclasts. The average sedimentation rate in the lower Pleistocene (23 to 24 m/m.y.) is identical to the rate for the entire Pleistocene, but it is twice as high as that estimated for the upper Pliocene (see next section).

Upper Pliocene (Fig. 7)

The 7-m-thick sediment sequence just above the hiatus corresponds to an upper Pliocene interval between 1.6 and 2.15 Ma in age, tentatively correlated with the Q and P zones of the Me-

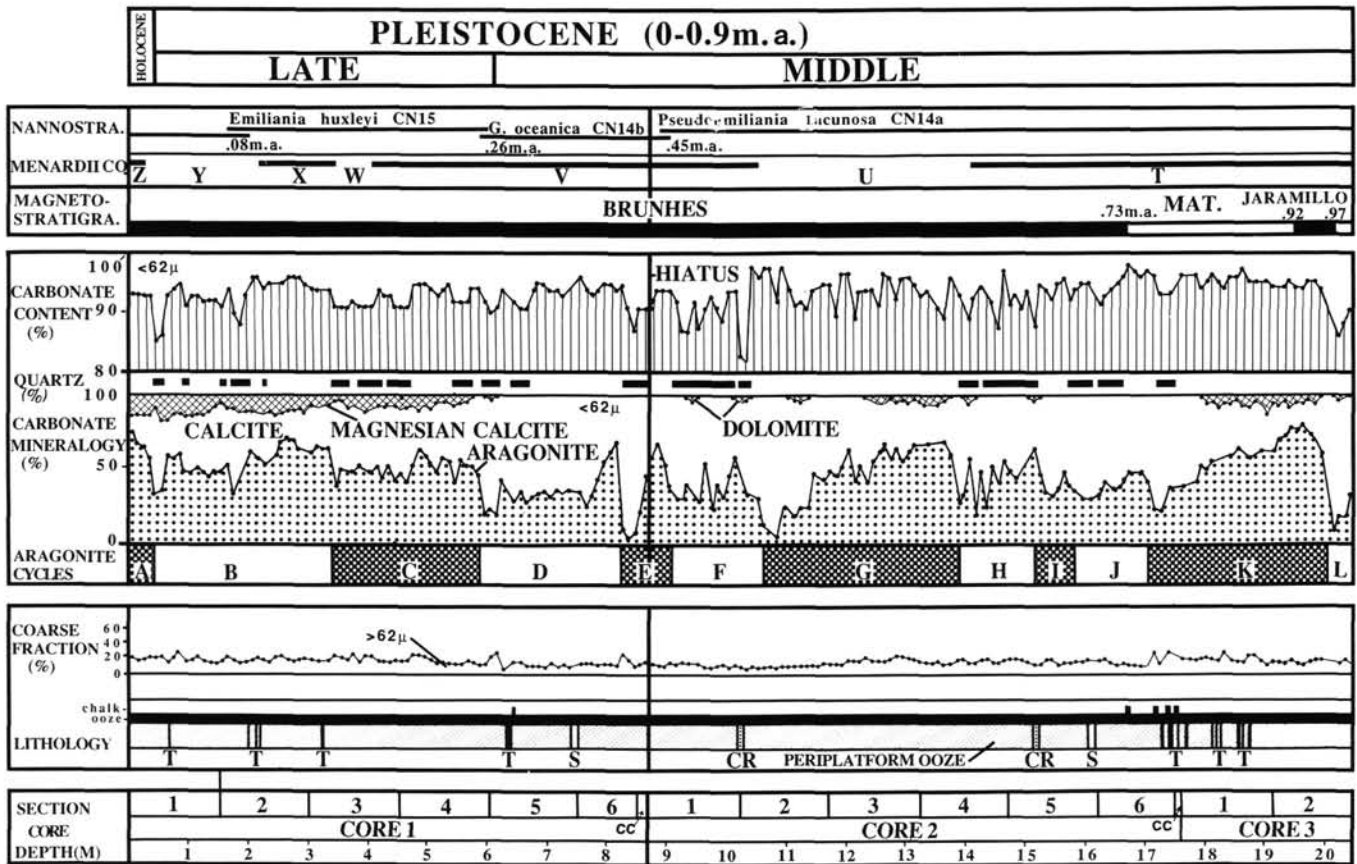


Figure 5. Depth variations of lithology, coarse fraction, carbonate mineralogy, quartz occurrence, and carbonate content within the Holocene through upper and middle Pleistocene (based on magnetostratigraphy), Menardi Complex, and nanno-stratigraphies with identification of 10.5 aragonite interglacial/glacial cycles labeled (from core top) A through K. Lithologic abbreviations: T, turbidite; CR, clay-rich layers; S, organic matter or interstitial-water samples.

nardi Complex. It is composed of almost pure periplatform ooze with only a single turbidite layer. Less than 10% of the sediment is indurated enough to be called a chalk.

Carbonate content in the fine fraction fluctuates between 84% and 100%, and the intervals of relatively low carbonate content correspond to layers in which quartz is observed on X-ray diffractograms. The range of upper Pliocene carbonate values resembles the Pleistocene carbonate fluctuations and differs from the fairly constant high average lower Pliocene carbonate values described below.

Aragonite and calcite are the two carbonate phases in the fine fraction. Aragonite content varies between 0% and 50%. Approximately half of the sediment is purely calcitic and therefore only pelagic in origin (Fig. 8C). Aragonite-bearing intervals are always relatively high in carbonate, although intervals with high carbonate values do not always correspond to those with aragonite. This is a major difference from what is generally observed in the upper Pleistocene: high carbonate corresponding to high aragonite, and vice versa (Droxler et al., 1983).

The coarse fraction varies from 10% to 50%. Intervals where coarse-fraction values reach 20% or more are mainly composed of agglomerates, microclasts, and foraminifer tests with calcite overgrowths. These intervals correspond to low-carbonate and low-aragonite or aragonite-free intervals. The average sedimentation rate (11 to 12 m/m.y.) during the late Pliocene, calculated using both nanofossil biostratigraphy and magnetostratigraphy (Figs. 3 and 4), is one of the lowest in the Pliocene-Pleistocene sequence. This interval of low sedimentation rate also cor-

responds to intermittent occurrence of aragonite and long sections of pure calcite.

Lower Pliocene (Fig. 7)

Sediment in the lower Pliocene interval between 3.75 and 4.45 Ma is a periplatform ooze/chalk devoid of turbidite layers. Approximately 40% of the ooze is sufficiently indurated to be considered a chalk. Carbonate content of the fine fraction is very high, generally greater than above the hiatus (upper Pliocene-Quaternary), and remains fairly constant between 93% and 99%. Absence of quartz on the X-ray diffraction diagrams demonstrates that the terrigenous input during the early Pliocene is either nonexistent or too small to be detected by our analytical methods. Three carbonate phases are present in the fine fraction: aragonite, calcite, and dolomite. Aragonite and calcite are the two major components, with dolomite quantitatively of secondary importance. In the bottom half of Core 101-633A-6H, aragonite content is as high as in Pleistocene interglacial maxima intervals from piston cores (Droxler et al., 1983; Boardman et al., 1986) and fluctuates between 50% and 70% (average 60%). Aragonite content fluctuates between 30% and 60% (average 45%) in the upper half of Core 101-633A-6H and varies between 0% and 40% (average 20%) in Sections 101-633A-5H-6 and 101-633A-5H-7. In summary, the aragonite content of the lower Pliocene section decreases incrementally upward. It is significant that high sedimentation rates (28 m/m.y.) prior to 4.25 Ma (Nunivak event, Fig. 4) correspond to an interval of high, fairly constant aragonite content, whereas low sedimentation

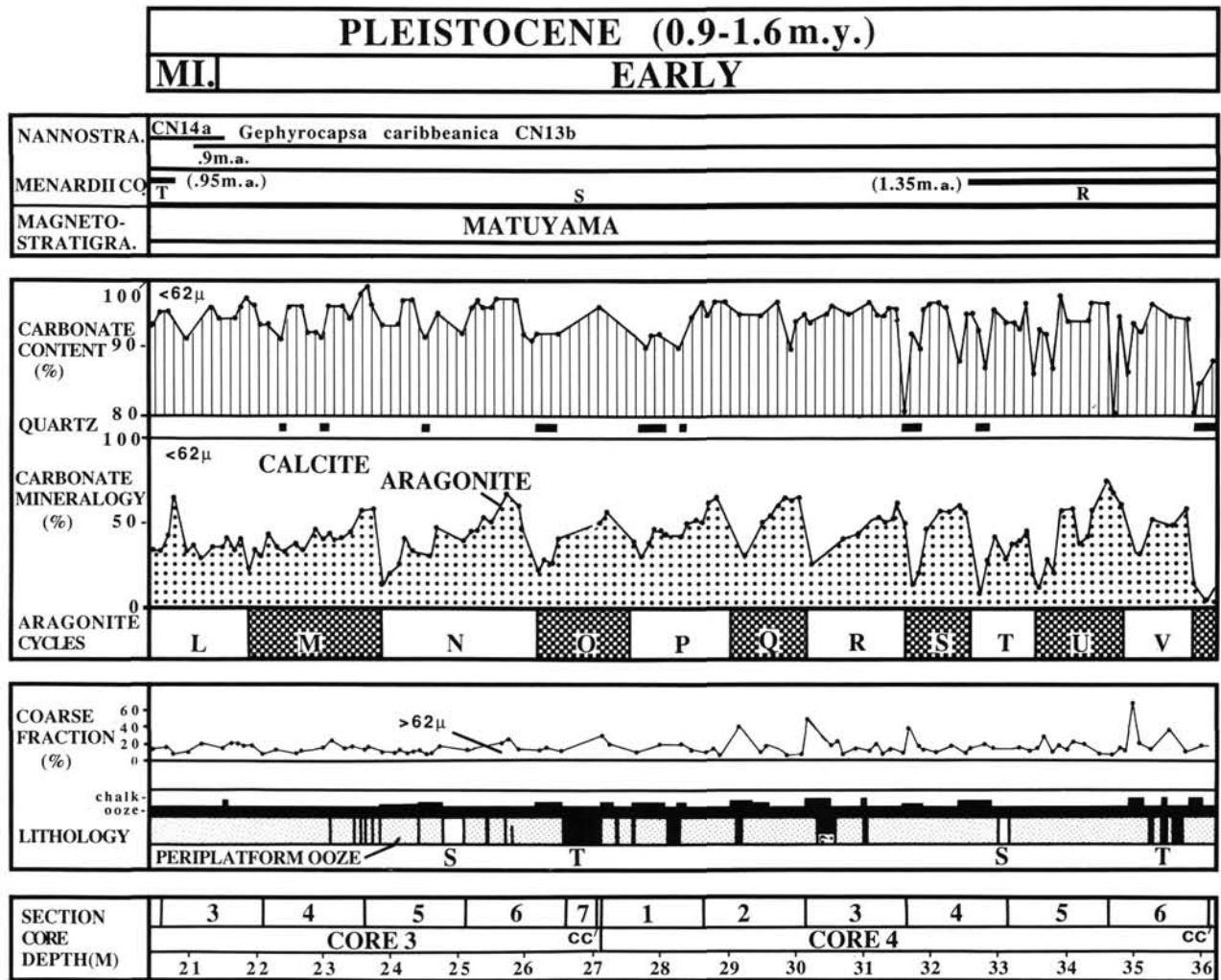


Figure 6. Depth variations of lithology, coarse fraction, carbonate mineralogy, quartz occurrence, and carbonate content within the lower Pleistocene (based on magnetostratigraphy), Menardii Complex, and nanno-stratigraphies with identification of 11 aragonite interglacial/glacial cycles labeled (from core top) L through V. (See Figure 5 caption for lithologic abbreviations.)

rates (10 m/m.y.) between 3.75 and 4.25 Ma coincide with a period of incremental drop of aragonite content in samples from the 7 m of sediment just below the hiatus.

Dolomite is always <8% throughout this interval, with the exception of Section 101-633A-5H-6 (immediately below the hiatus), where dolomite constitutes as much as 25% of the total carbonate. Observations by SEM show that the sediment is composed mainly of easily identifiable coccolith plates, as well as recrystallized(?) material with some needlelike individual particles that are interpreted as being aragonitic on the basis of X-ray-diffraction analyses. Dolomite appears as clear rhombs 10 to 20 μm in size within the fine matrix, and is therefore interpreted (Mullins et al., 1985) to be authigenic and diagenetically produced (Fig. 8, A and B). The dolomite precursor could have been some bank-derived diagenetically metastable magnesian calcite, which usually occurs intermittently in the upper and middle Pleistocene. However, it is not clear that dolomite is formed by recrystallization of magnesian calcite, since both dolomite and magnesian calcite are commonly absent simultaneously in the Pliocene-Pleistocene periplatform ooze.

The sudden decrease of the coarse fraction in the middle of Section 101-633A-6H-3 from an average of 50% to less than 20% is evidently the result of diagenetic processes. The coarse

fraction in the bottom half of Core 101-633A-6H is composed primarily of agglomerates and cemented clasts, and not only of foraminifer tests as it is in the case in the top half of Core 101-633A-6H, where the coarse fraction is <20% of the total sediment.

Overall Pliocene-Pleistocene Trends in Carbonate Content, Carbonate Mineralogy, and Coarse-Fraction Proportions

Average values of carbonate content are close to 100% and mostly constant in Hole 633A in the lower Pliocene (43.75 to 55.00 mbsf) and in the upper half of the lower Pleistocene. These values are somewhat lower and characterized by rapid excursions to relatively low values (down to 77%) in the rest of the Pleistocene and the upper Pliocene. It is therefore significant that the lower Pliocene interval represents a time during which terrigenous input was at its minimum or was nonexistent.

Results of the carbonate mineralogical studies show irregular aragonite fluctuations and indistinct aragonite cycles in the upper Pliocene and well-developed and clearly asymmetric aragonite cycles throughout the Quaternary. Surprisingly, the highest and most constant aragonite values occur in the lower Pliocene; these values decrease by several steps within just a few meters below the Pliocene hiatus.

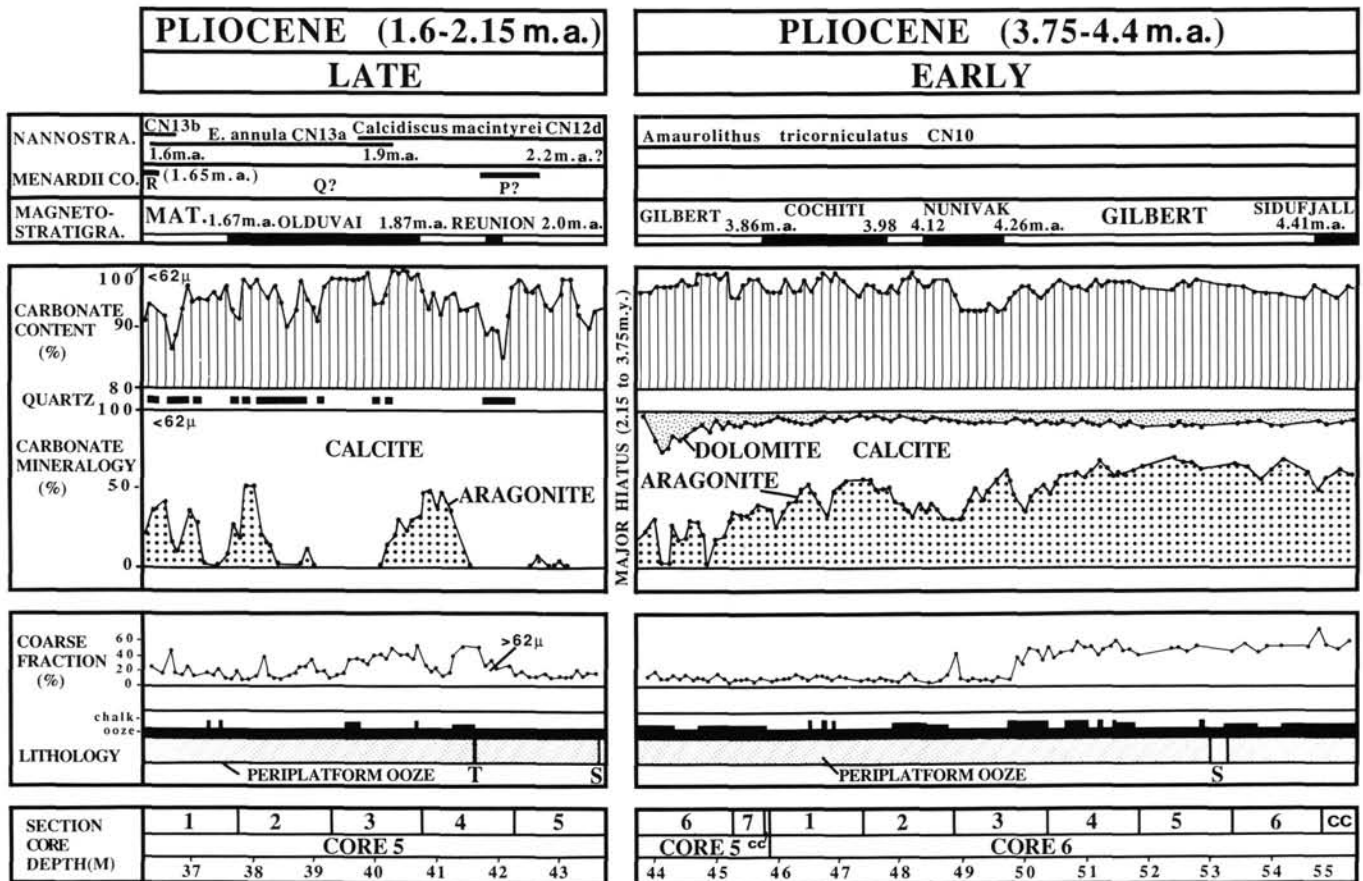


Figure 7. Depth variations of lithology, coarse fraction, carbonate mineralogy, quartz occurrence, and carbonate content within the Pliocene (based on magnetostratigraphy), Menardii Complex, and nanno-stratigraphies. (See Figure 5 caption for lithologic abbreviations.)

Magnesian calcite as a secondary mineral reaches maximum values at the top of Hole 633A, then decreases downhole and disappears at 6 mbsf. It reappears only in two well-developed aragonite-rich intervals. Dolomite as a secondary mineral is also ubiquitous in the lower Pliocene and appears only as traces in association with clay-rich layers in the Pleistocene. The highest proportions of the coarse-sized fraction ($>20\%$) correspond to evidences of partial cementation in microclasts, and calcite overgrowths in foraminiferal tests occur in the upper Pliocene and the lower half of the lower Pliocene, where aragonite values are usually constant and high ($\sim 60\%$).

Pliocene-Pleistocene Oxygen-Isotope Record and Its Correlation with Variations in Aragonite Content

We have produced an almost complete oxygen-isotope planktonic record using *Globigerinoides sacculifera* and *Globigerinoides rubra* (pink) in the top 47 m of Hole 633A. This record includes the past 2.15 m.y. above the Pliocene hiatus at 43.75 mbsf, and a time interval between 3.75 and 3.9 Ma in the 3.5 m of periplatform ooze just below the hiatus. The results are shown in Figure 9 (Pleistocene), Figure 10 (Pliocene), and the Appendix.

Oxygen-Isotope Planktonic Record (Figs. 9 and 10)

The Pleistocene oxygen-isotope record (top 36.50 m of Hole 633A) clearly displays its two commonly observed modes: low-frequency/high-amplitude cycles in the upper and middle Pleistocene (Brunhes Chron and Matuyama Chron to Jaramillo Event, 0.97 Ma to present) and high-frequency/low-amplitude cycles in the lower Pleistocene (in the Matuyama Chron from

the top of the Olduvai Event to the bottom of the Jaramillo Event, 1.67 to 0.97 Ma). These two modes were observed by Shackleton and Opdyke (1976) in the Pacific Ocean (core V28-239), by Prell (1982) in the Caribbean Sea (DSDP Hole 502B), and by Shackleton et al. (1984) in the North Atlantic Ocean (DSDP Hole 552A). In Hole 633A, the maximum glacial/interglacial amplitudes in the lower Pleistocene mode fall, with a few exceptions, within a range of values between 0.5% and -1.5% , whereas in the middle/upper Pleistocene mode, values of maximum amplitudes range between 1.3% and -2.0% .

Identification of the successive oxygen-isotope stages for the late Pleistocene is not straightforward. However, using the biostratigraphic markers based on nannofossils, the Menardii Complex zones, and the magnetic reversals, we tentatively identify the 23 oxygen-isotope stages defined by Shackleton and Opdyke (1976) in piston core V28-239. In our interpretation of the oxygen-isotope record of Hole 633A, as in piston core V28-239, the Brunhes/Matuyama reversal lies on the stage 20/21 boundary, and the top of the Jaramillo Event falls in stage 23. As globally recorded for the late and middle Pleistocene (Thierstein et al., 1977), the last-occurrence datum (LAD) of *Pseudoemiliania lacunosa* is located in stage 12, the first-occurrence datum (FAD) of *Emiliania huxleyi* in stage 8, and the beginning of the *E. huxleyi* acme zone at the end of stage 5. In addition, as in core V16-205 from the tropical Atlantic Ocean (Van Donk, 1976), the Z Zone of the Menardii Complex corresponds to the Holocene or stage 1; the Y and X zones roughly to stages 2 to 4 and stage 5, respectively; the W Zone to stage 6; the V Zone from stages 7 to 13; the U Zone from stages 14 to 15; and, finally, the T zone from stages 16 to 23.

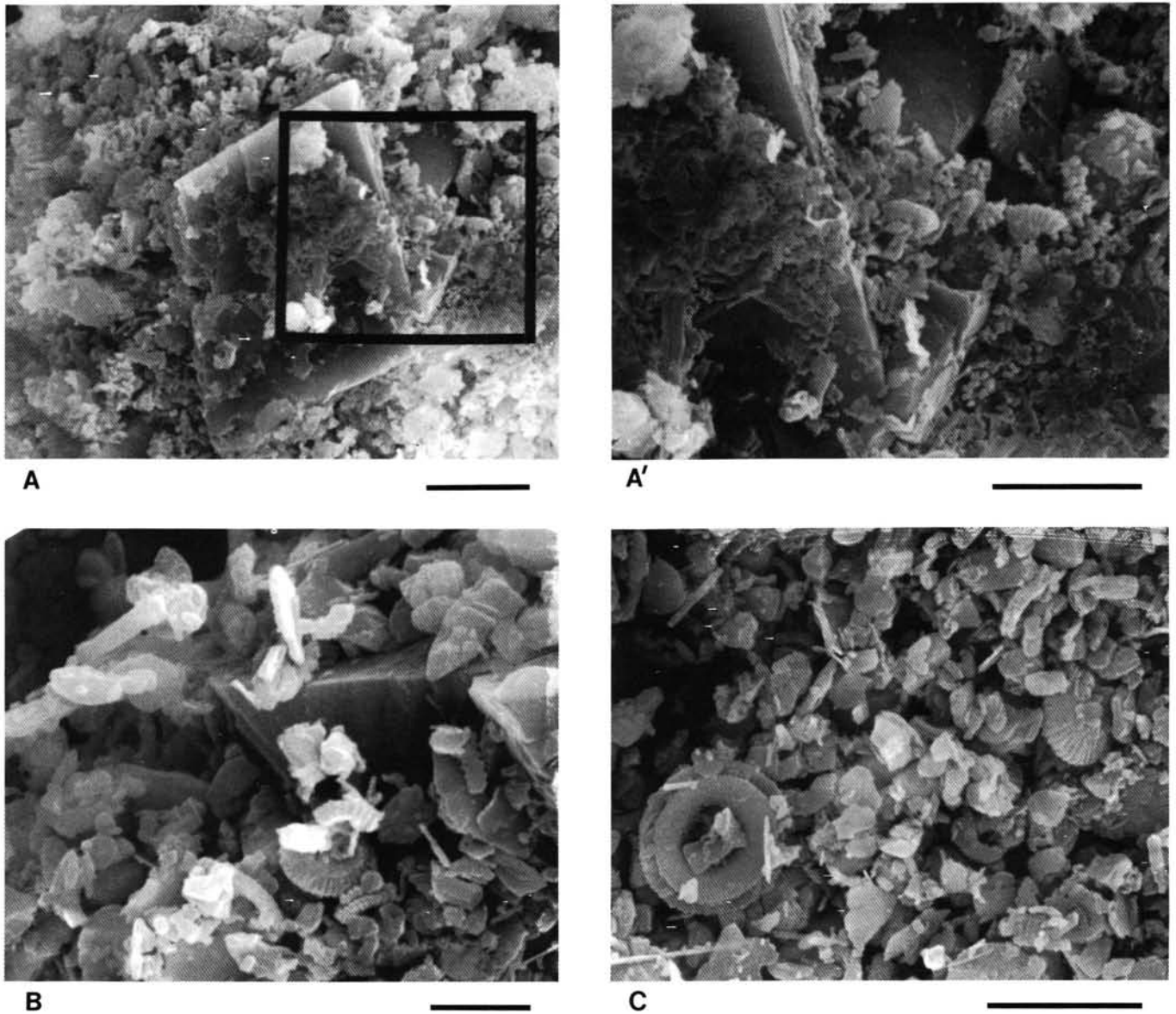


Figure 8. SEM photomicrographs of Pliocene periplatform carbonate ooze. A. Sample 101-633A-6H-6, 85–87 cm; dolomite rhomb growing within a matrix of coccolith plates and recrystallized(?) aragonite particles, some still appearing as needles; bar = 5 μm ; $\times 3000$. A'. Detail of micrograph A; bar = 2.5 μm ; $\times 7000$. B. Sample 101-633A-5-6, 34–35 cm; dolomite rhomb growing within a matrix of pure calcitic particles, mainly coccolith plates and undifferentiated grains; bar = 2.5 μm ; $\times 5500$. C. Sample 101-633A-5-5, 134–135 cm; pure calcitic ooze, mainly coccolith plates and some undifferentiated grains; bar = 5 μm ; $\times 4500$.

As in other records, glacial stages 12, 16, and 22 in Hole 633A (middle Pleistocene) are among the heaviest oxygen-isotope values, and interglacial stages 17, 19, and 21 are the least developed. Glacial stage 14, usually characterized by relatively light oxygen-isotope values, shows oxygen values in Hole 633A as heavy as those during stage 12. The beginning of interglacial stage 5 (5e) seems to be partly missing; a small hiatus could be induced by the occurrence of a turbidite layer at that level (3.20 to 3.30 mbsf). In addition, the glacial/interglacial record loses its resolution between stages 11 and 12, which coincides with the transition between Cores 101-633-1H and 101-633-2H and therefore could be related to drilling disturbances. The general pattern of the oxygen-isotope record in Hole 633A in the upper and middle Pleistocene is somewhat peculiar, as some of the interglacial stages are extended (i.e., stages 15 and 23). Sedimen-

tation rates in the Bahamas are reported to be much higher for the late Pleistocene than during glacial stages by a factor of 4 to 8 (Droxler et al., 1983; Boardman and Neumann, 1984; Droxler and Schlager, 1985a; Reymer et al., this volume). This may be because of preferential highstand input of bank-derived carbonates and possibly because of preferential interglacial aragonite preservation. This contrasts with the open ocean, where the glacial record may be extended, owing to preferential terrigenous input during a lowstand interval.

The difficulty in identifying clear glacial/interglacial stages in the lower Pleistocene can be explained by their higher frequency and lower amplitude. In Hole 633A, upper Pliocene oxygen-isotope values are similar to those from the lower Pleistocene. This differs from the oxygen-isotope record of DSDP Hole 552A, where glacial/interglacial cycles in the upper Plio-

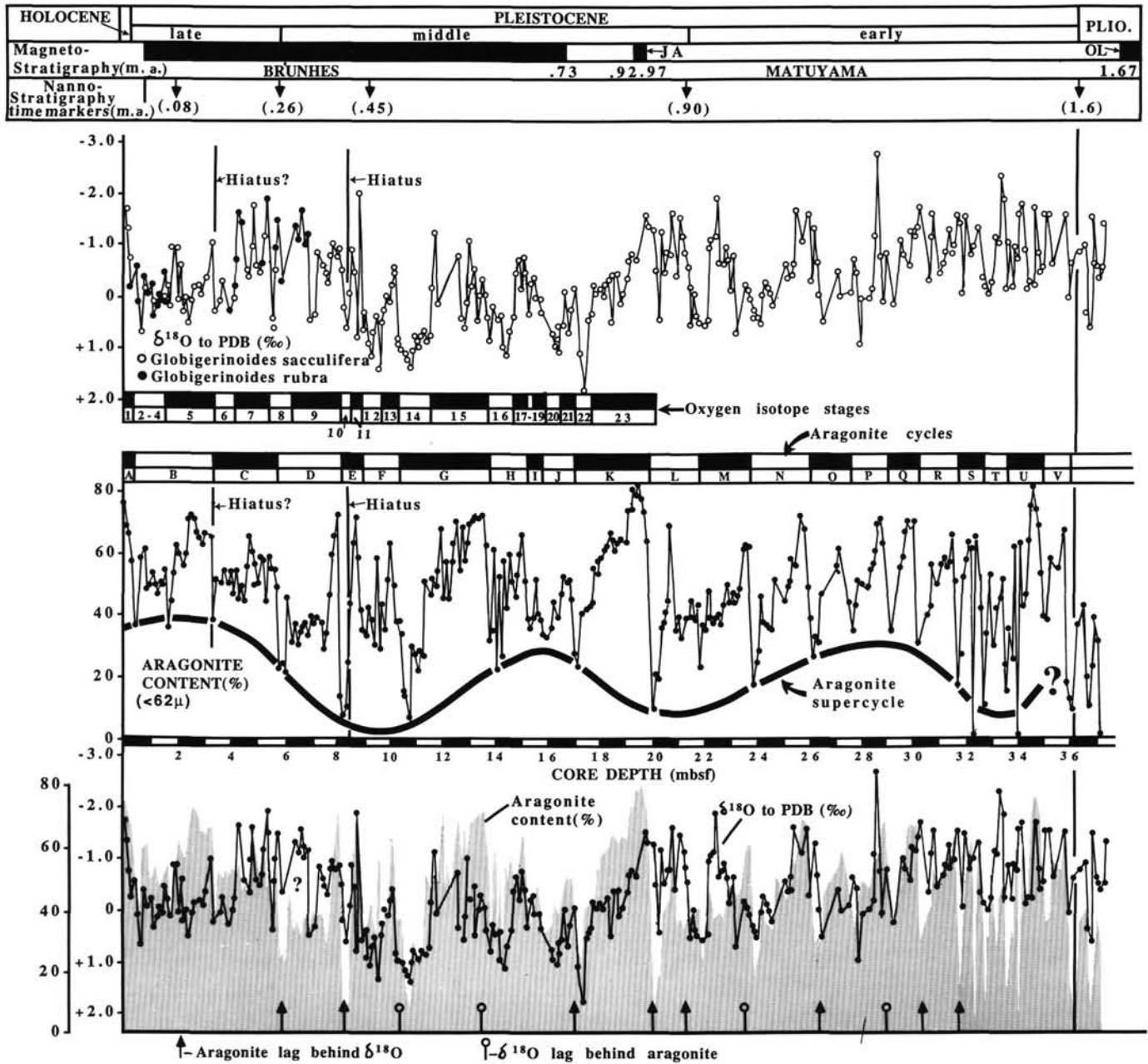


Figure 9. Quaternary oxygen-isotope planktonic record (upper diagram) and aragonite cycles and supercycles in fine-sediment fraction ($<62 \mu\text{m}$) (middle diagram). Records are superimposed for easier visual comparison (lower diagram) and placed on a time scale based on magneto- and nannostratigraphic time markers. Twenty-three oxygen-isotope stages are identified within the first 1 m.y. (Holocene, upper and middle Pleistocene). Twenty-one and one-half aragonite cycles (each cycle including one interglacial and one glacial interval) are identified (from core top down) and labeled A through V. (See text for general description and discussion.)

cene are more upper Pleistocene-like with generally intermediate amplitudes (Shackleton et al., 1984).

The short $\delta^{18}\text{O}$ record in the lower Pliocene (3.9 to 3.75 Ma) just below the hiatus first shows a steep decrease of oxygen values by 2.2‰, followed by a plateau with an average value of 0‰. The timing (~ 3.8 Ma) of this climatic deterioration fits well with the interpretation that the early Pliocene was a prolonged interval of warm interglacial conditions starting around 5 Ma, which ended at 4.1 Ma with a sharp climatic cooling (Hodell and Kennett, 1986). The sea-level curve of Haq et al. (1987) also shows a sharp drop between 4.0 and 3.8 Ma.

Correlations Between Aragonite Cycles and Oxygen-Isotope Record

Quaternary (Holocene-Pleistocene, 0–1.6 Ma) (Fig. 9)

In this paper we visually compare the oxygen-isotope record and the aragonite cycles. In Figure 9, the oxygen-isotope record and the aragonite cycles are displayed both separately and superimposed to facilitate the comparison.

Excellent correlations between the $\delta^{18}\text{O}$ record and aragonite cycles in the upper Pleistocene and part of the middle Pleistocene were found by Droxler et al. (1983). Their study examined

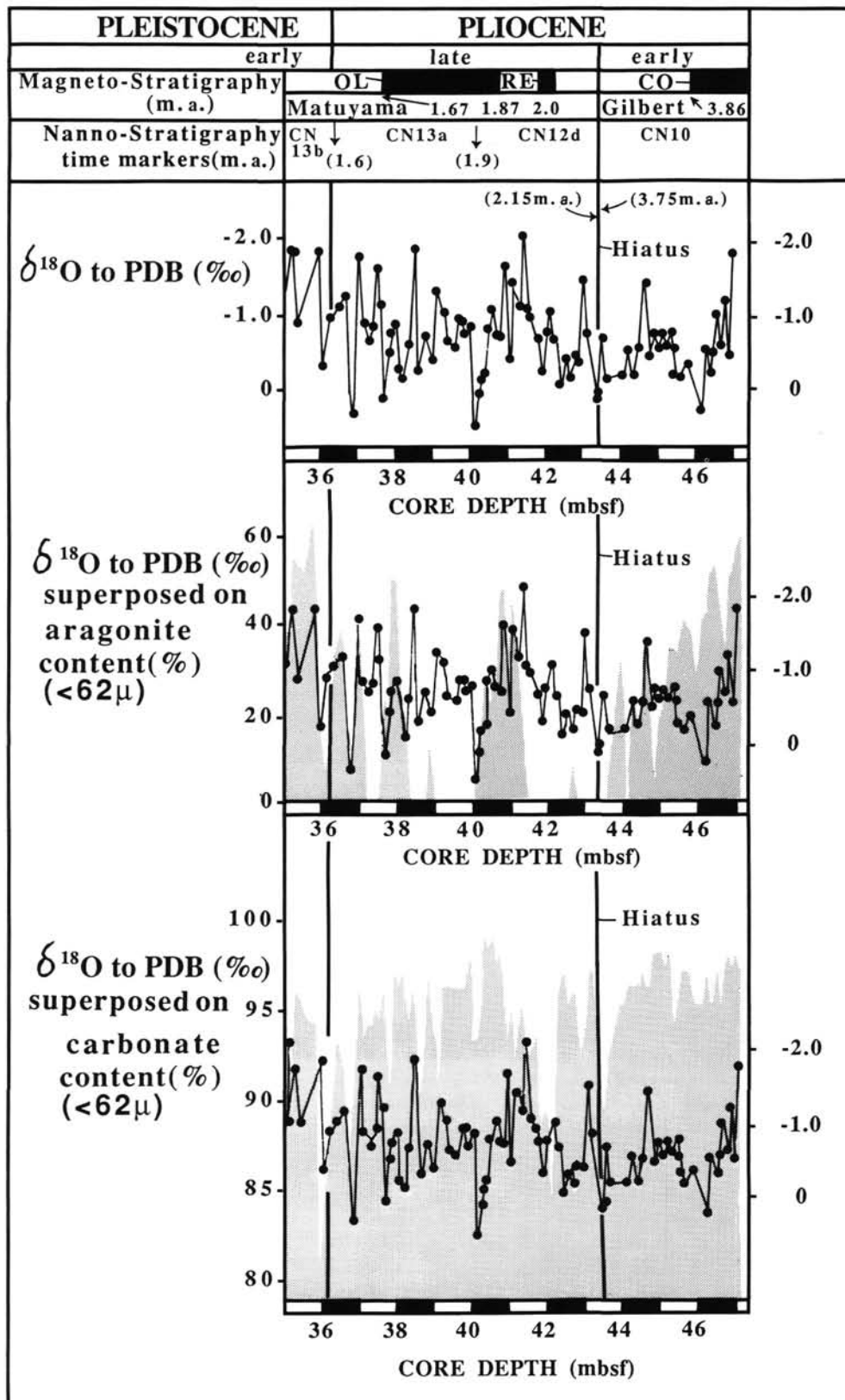


Figure 10. Pliocene oxygen-isotope planktonic record (upper diagram), superimposed on aragonite variations (middle diagram) and on carbonate variations (lower diagram). Note that in the upper Pliocene a good correlation exists between the oxygen-isotope record and carbonate cycles, whereas irregular low values of aragonite, or intervals characterized by absence of aragonite, show no clear relationship with either the oxygen-isotope record or the carbonate cycles. In the lower Pliocene the aragonite decrease corresponds to a distinct increase of oxygen-isotope values, and carbonate values remain high and constant. (See text for general description and discussion.)

piston core GS-7705-34, taken in Tongue of the Ocean (1935 m water depth) and containing a record of the past 0.35 m.y. (similar to Hole 633A). Kiefer (1983) and Boardman et al. (1986) report similar results from piston core CH-8201-07, Northwest Providence Channel (675 m water depth), which contains a record of the past 0.50 m.y. (Kiefer, 1983; Boardman et al., 1986). More recent research on periplatform ooze from the Nicaragua Rise (Caribbean Sea) and from the Maldives (Indian Ocean) has confirmed the correlation between the aragonite cycle and oxygen-isotope record during the past 0.35 m.y. (Droxler, 1986a).

The general visual correlation between aragonite content and $\delta^{18}\text{O}$ in the much longer record of Hole 633A is quite good, in spite of several mismatches that might be significant in interpreting the origin of the aragonite cycles. In Core 101-633A-1H (0–8.7 mbsf), covering the Holocene, upper Pleistocene, and part of the middle Pleistocene (0–0.45 Ma), the correlations between $\delta^{18}\text{O}$ and the aragonite cycles are not as clear as in the other records from piston cores (Droxler et al., 1983; Boardman et al., 1986; Droxler, 1986a). A possible hiatus at the beginning of isotope stage 5 (5e), equivalent to aragonite cycle B, as well as in isotope stage 11, equivalent to aragonite cycle E can partially explain some of the discrepancies between $\delta^{18}\text{O}$ and the aragonite cycles (although the latter example may be related to drilling disturbances at the transition between Cores 101-633A-1H and 101-633A-2H). In addition, long and frustrating analytical problems arose during oxygen-isotope analysis of samples from the top 7 m of Core 101-633A-1H; duplicate and even triplicate analyses (some based on *Globigerinoides rubra*) had to be run to resolve some of the discrepancies.

Mismatches between the oxygen-isotope record and the aragonite cycles seem to occur at several glacial-to-interglacial transitions, where the aragonite increase lags behind the $\delta^{18}\text{O}$ depletion. The most obvious cases are boundaries 10 to 9 (E/D), 12 to 11 (F/E), 22 to 21 (K/G), and 24 to 23 (L/K) in the middle Pleistocene, and several cases in the lower Pleistocene, at boundaries M/L, O/N, R/Q, and S/R. In a few instances, the opposite seems to occur; the aragonite increase precedes the $\delta^{18}\text{O}$ depletion at the boundaries H/G, N/M, and Q/P. More detailed studies based on closer sampling (3- to 5-cm-spaced samples) of these particular glacial-to-interglacial boundaries will be necessary in order to quantify and to better understand the lags between the aragonite increase and the $\delta^{18}\text{O}$ depletion at the glacial-to-interglacial transitions.

Pliocene (Fig. 10)

The correlation between the $\delta^{18}\text{O}$ record and the aragonite curve is more tenuous in the upper Pliocene (1.6 to 2.15 Ma) than in the Quaternary (0 to 1.6 Ma). Although the Pliocene oxygen-isotope cycles are almost identical to the lower Pleistocene cycles in terms of amplitude and frequency, aragonite is not always present, and the correspondence between $\delta^{18}\text{O}$ and the aragonite curve is not always straightforward. Interglacial (light-oxygen-isotope) intervals may correspond to aragonite-rich intervals but can in other cases coincide with pure calcitic ooze. Although the glacial/interglacial mode during the late Pliocene is well established after the onset of major glaciations in the North Atlantic Ocean 2.4 m.y. ago in DSDP Hole 552A (Shackleton et al., 1984), as well as in DSDP Hole 502B (Prell, 1982) and now in Hole 633A, occurrence of climatically induced aragonite cycles remains unclear in the upper Pliocene. The climatically induced aragonite cycles start at the Pliocene-Pleistocene transition, 1.6 m.y. ago at 36.5 mbsf in Hole 633A, and are fully developed, displaying a good correlation with the $\delta^{18}\text{O}$ planktonic record throughout the Quaternary.

The short lower Pliocene $\delta^{18}\text{O}$ record and the aragonite curve in the 3 m of sediment just below the Pliocene hiatus are significant. Comparison of the records shows that the $\delta^{18}\text{O}$ increase of

2.2‰ at around 3.8 Ma, which might represent the well-established climatic deterioration between 3.9 and 3.75 Ma (Hodell and Kennett, 1986; Haq et al., 1987), parallels a fairly sharp decrease of aragonite content (from 55% to 25%).

DISCUSSION

The detailed study of the top 55 m in Hole 633A has extended the aragonite record much farther back in time than we thought possible before Leg 101. Hole 633A contains a nearly complete high-resolution Quaternary record, and in spite of a 1.6-m.y.-long hiatus, its partial Pliocene record bears important findings.

Quaternary Aragonite Cycles

Asymmetric aragonite cycles are developed throughout the entire Quaternary sequence and are well correlated with a planktonic oxygen-isotope record. The aragonite record, as is already well established for the oxygen-isotope record, displays high-frequency cycles (one cycle every 50,000 yr, 11 cycles, L through V, in 0.6 m.y.), in the lower Pleistocene whereas in the middle and upper Pleistocene, relatively low frequency cycles occur (one cycle every 100,000 yr, 10.5 cycles, A to K, in 1.0 m.y.). Aragonite maxima remain fairly constant throughout the Pleistocene (averaging ~40%). The amplitude of the sharp aragonite increase at each cycle boundary can be as high as 75% and as low as 25%. It is significant, however, that the large-amplitude variations of the aragonite cycles do not occur at random but seem to be organized within a roughly 0.5-m.y. supercycle. This supercycle includes three intervals characterized by extremely low aragonite values at (1) 0.3 to 0.5 Ma, within the mid-Brunhes centered at the LAD of *Pseudoemiliania lacunosa*; (2) 0.9 to 1.0 Ma, within the Jaramillo Event; and (3) 1.4 to 1.5 Ma (just above the Pliocene/Pleistocene contact). One-half of the last 0.5-m.y.-long aragonite supercycle has been observed in at least four cores, collected in water depths ranging between 1200 and 2000 m, from two Bahamian basins. Figure 11A shows a plot of average aragonite values for the last four glacial intervals, corresponding to isotope stages 2 through 4, 6, 8, and 10, during the last 0.35 m.y. in two piston cores from Tongue of the Ocean, P-7102-14 (Droxler, 1984) and GS-7705-34 (Droxler et al., 1983), and in ODP Holes 632A (Reymer et al., this volume) and 633A (this chapter). In the four cores, aragonite values are minimum during isotope glacial stage 10 and maximum during isotope stage 6.

The aragonite supercycles look suspiciously similar to low-frequency carbonate Quaternary cycles (wavelength on the order of 0.5 m.y.), observed in the equatorial Pacific Ocean by Hays et al. (1969), Saito et al. (1975), and Adelseck (1977); in the north-central Pacific Ocean (Vincent, 1985); in the equatorial Indian Ocean (Peterson and Prell, 1985); and in the North Atlantic (Crowley, 1985). The three intervals of lowest aragonite values during the Quaternary in Hole 633A correspond chronologically quite well to three intervals of very low carbonate values defined in three Pacific cores (RC-11-209, V-24-58, and RC-12-66): (1) the middle Brunhes minimum (B5 to B11), (2) the Jaramillo minimum (M1 to M7), and (3) the middle Matuyama minimum (M11 to M13) (Hays et al., 1969; Saito et al., 1975; Vincent, 1985). The last middle Brunhes carbonate minimum has been shown to occur worldwide and has been interpreted to be directly caused by a global increase of carbonate dissolution, which was observed in the Pacific Ocean by Adelseck (1977), in the Indian Ocean by Peterson and Prell (1985), and in the Atlantic Ocean by Crowley (1985).

Because the timing of the 0.5-m.y.-long Quaternary carbonate dissolution cycles is so close to the timing of the aragonite supercycles in Hole 633A, we are tempted to interpret by analogy the aragonite supercycles as dissolution cycles at intermedi-

Tongue of the Ocean

- GS 7705-34 (Droxler et al., 1983)
● P 7102-14 (Droxler, 1984)

Exuma Sound

- △ ODP Hole 633A (this paper)
▲ ODP Hole 632A (Reymer et al., this vol.)

■ Pteropod ratio = $\frac{\text{whole tests}}{\text{whole \& fragmented tests}}$

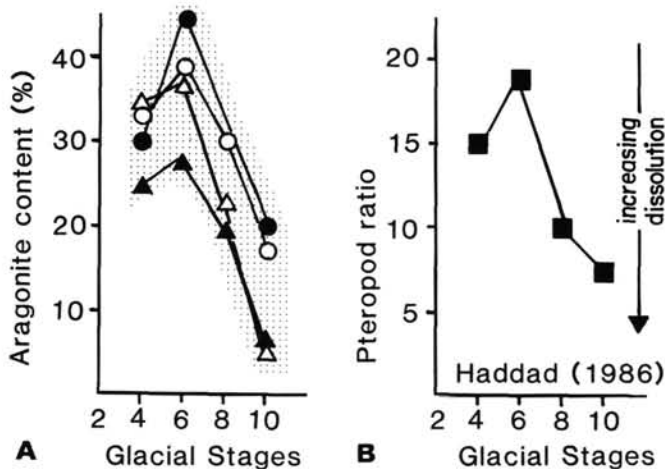


Figure 11. A. Last half of aragonite supercycle recorded in four Bahamian cores by the variations of the average aragonite values for the last four glacial aragonite minima (glacial isotope stages 2 through 4, 6, 8, and 10). Note the lowest average values during stage 10 and the highest aragonite values during stage 6. B. Pteropod ratio (whole tests/whole and fragmented tests), possible dissolution index, for the last glacial isotope stages 2 through 4, 6, 8, and 10. Note minimum number of whole pteropod tests (maximum dissolution) during stage 10 and maximum number of whole pteropod tests (minimum dissolution) during stage 6.

ate water depth. Direct evidence is, however, needed to strengthen our interpretation. Haddad (1986), studying pteropod occurrence and degree of preservation, has shown in a core from Northwest Providence Channel (water depth, 675 m) that values of the ratio between the number of whole tests over the number of whole and fragmented tests vary downcore. This ratio can be used as a dissolution indicator in analogy with foraminifer studies using whole tests and fragments. We have plotted in Figure 11B Haddad's data for the last four glacial stages, corresponding to the last half of the aragonite supercycle; Stage 10 shows maximum values of pteropod dissolution corresponding to the lowest aragonite minimum values in four other Bahamian cores, whereas Stage 6 shows minimum dissolution values corresponding to the highest values of aragonite minimum in the four cores (see Fig. 11A and B).

During the Quaternary, the planktonic oxygen-isotope record correlates well with the aragonite cycles. Some mismatches generally appear at glacial-to-interglacial boundaries, where the aragonite increase lags behind the oxygen-isotope depletion most of the time, or vice versa (Fig. 9). The significance of these lags is incompletely understood, and further studies are needed to positively confirm their existence. These lags could, however, become highly significant in solving the controversy over the origin of the climatically induced aragonite cycles. The question remains whether the cycles reflect a pure aragonite input signal related to bank flooding (i.e., Boardman and Neumann, 1986) or a combination of both an aragonite input and preservation

(caused by changing the aragonite saturation level within the water columns in relation to climatically induced variations of the carbonate chemistry in intermediate water masses). We are tempted to interpret these lags between aragonite increase and oxygen depletion by temporary decoupling of aragonite input and preservation/dissolution signal, especially in the case where a (0.5-m.y.) preservation/dissolution supercycle is added to the high-frequency cycles. Statistical analyses of the different signals and further detailed studies of the lags between the different signals need to be developed to address these problems.

Pliocene Aragonite Record

In spite of the 1.6-m.y.-long hiatus, the incomplete Pliocene record in Hole 633A is somewhat puzzling, since it displays the lowest and the highest values of aragonite content observed in the entire Pliocene-Pleistocene record.

The upper Pliocene sequence of Hole 633A includes only the interval between 2.15 and 1.6 Ma. This corresponds to a time just following the onset of major glaciation in the North Atlantic, dated at 2.4 Ma by Shackleton et al. (1984). The Hole 633A sequence is characterized by generally low aragonite content and commonly a total absence of aragonite. In addition, the aragonite variations are irregular. They display no distinct cyclic pattern, although the planktonic oxygen-isotope record for the same interval shows high-frequency and relatively low-amplitude climatic cycles, similar to the early Pleistocene cycles. There is therefore no clear correlation between the oxygen-isotope cycles and the irregular aragonite variations, as was the case later during the early Pleistocene, when aragonite cycles were well developed. In the same upper Pliocene interval, the fluctuations in carbonate content are the largest recorded during the entire Pliocene-Pleistocene, except for the two clay-rich layers in the middle Pleistocene. This observation seems logical because the upper Pliocene interval was deposited just after the onset of the major glaciations in the North Atlantic. Furthermore, carbonate fluctuations are known to be related in the Bahamas, at least during the late Pleistocene, to variable rates of dilution by glacial input of fine terrigenous material transported southward by the Western Boundary Undercurrent (Droxler, 1984). In addition, the carbonate fluctuations correlate well with the oxygen-isotope record, with low carbonate values (quartz occurrence) corresponding to glacial heavy oxygen-isotope values. Absence or low content of aragonite and a lack of cyclic pattern in the aragonite content are surprising, since both the oxygen-isotope and the carbonate records show an early-Pleistocene-like glacial cyclic pattern.

The late Pliocene aragonite record can represent either a temporary cutoff of the primary input of bank-derived aragonite or a generally poor preservation (greater dissolution) of the aragonite at the seafloor. The amplitude and frequency of the oxygen-isotope cycles (a proxy to the sea-level curve) remained similar during the late Pliocene and early Pleistocene, whereas the aragonite cycles were initiated only at the Pliocene/Pleistocene boundary. Thus it is difficult to imagine an almost complete cutoff of aragonite input to explain the low values or absence of aragonite during the late Pliocene. On the other hand, in several carbonate curves published by Hays et al. (1969), Saito et al. (1975), and Vincent (1985), the late Pliocene interval centered on the Olduvai Event generally corresponds to one of the most extreme carbonate minima (intense dissolution interval M17) for the entire Pliocene-Pleistocene. We are thus tempted to interpret the low values or absence of aragonite during the late Pliocene as evidence for dissolution of the bank aragonite at the seafloor.

The lower Pliocene sequence of Hole 633A is also incomplete. On the basis of magnetostratigraphy it is estimated to correspond to a time span between 4.5 and 3.75 Ma. Besides the presence of authigenic dolomite as a secondary mineral and a

general occurrence of chalk, both related to early sub-seafloor diagenesis, values of aragonite content are among the highest for the Pliocene-Pleistocene sequence of Hole 633A. The aragonite values remain fairly constant between ~4.50 to 4.25 Ma, a time interval characterized by the highest sedimentation rates (28 m/m.y.) recorded for the Pliocene-Pleistocene. The next interval (4.25 to 3.75 Ma) is characterized by an incremental drop of aragonite and low sedimentation rate, parallel with an enrichment of $\delta^{18}\text{O}$ between 3.9 and 3.75 Ma, corresponding to a well-established climatic deterioration (Hodell and Kennett, 1986; Haq et al., 1987) as well as a gradual decrease of carbonate preservation in equatorial Pacific cores (Hays et al., 1969; Saito et al., 1975; Vincent, 1985). Contrary to the large fluctuations of carbonate content in the late Pliocene, the carbonate values during the early Pliocene (prior to the onset of the major glaciations in the North Atlantic) are the highest among the Pliocene-Pleistocene cores and remain mostly constant.

CONCLUSIONS

The top 55 m of Hole 633A corresponds to the past 4.5 m.y., including a 1.6-m.y.-long Pliocene hiatus, constrained in time by calcareous-nannofossil biostratigraphy and magnetostratigraphy between 2.15 and 3.75 Ma. Downcore variations of aragonite content in the periplatform sequence of Hole 633A provide a detailed record of Pliocene-Pleistocene oceanographic changes of intermediate water masses. The aragonite paleoceanographic primary record remains surprisingly unaltered despite such early diagenetic processes as (1) rapid downcore disappearance of magnesian calcite; (2) partial calcite overgrowth and cementation in chalky intervals, more common in the deepest part of the sequence; and (3) ubiquitous occurrence of authigenic dolomite as a secondary mineral in the lower Pliocene.

Twenty-one and one-half (A through V) climatically induced cycles are observed throughout the entire Quaternary (past 1.6 m.y.). They correlate well with a planktonic-foraminifer oxygen-isotope curve established from the same set of samples. Each interglacial/glacial cycle starts with a sharp aragonite increase at the deglaciation transition, followed by a gradual aragonite decrease toward the glacial interval. As was well-documented in the Quaternary oxygen-isotope record, high-frequency aragonite cycles (approximately 1 cycle every 50,000 yr) during the early Pleistocene switch to low-frequency (approximately 1 cycle every 100,000 yr) aragonite cycles during the middle and late Pleistocene. Lower frequency aragonite supercycles (approximately 1 cycle every 0.5 m.y.) appear in the full aragonite Quaternary record. Their timing matches the low-frequency (1 cycle every 0.4 to 0.5 m.y.) carbonate dissolution/preservation cycle observed mainly in cores from the Pacific Ocean but also in the Indian and North Atlantic oceans.

The low values or absence of aragonite as well as the noncyclic aragonite variations in the late Pliocene (2.15 to 1.6 m.y.) are somewhat puzzling, since during the same period early Pleistocene-like oxygen-isotope cycles as well as carbonate-dilution cycles are well developed. The lack of aragonite cycles could be interpreted as particularly poor preservation of the aragonite input at the seafloor during the part of the late Pliocene within the normal Olduvai Event, an interval known in the equatorial Pacific as one with the poorest carbonate preservation during the Pliocene-Pleistocene. The early Pliocene interval between 4.5 and 4.25 Ma is characterized by very high and fairly constant aragonite content and high sedimentation rates (28 m/m.y.), and it corresponds to the end of a prolonged warm interglacial interval characterized by good carbonate preservation in the equatorial Pacific Ocean and quite high sea level. The incremental aragonite decrease between 4.25 and 3.75 Ma corresponds to a climatic cooling, to a step-like decrease of carbonate preservation in the equatorial Pacific Ocean, and to a global lowering of sea level.

Because of (1) good correlation between the oxygen-isotope record and the aragonite cycles, (2) occurrence of the aragonite supercycle, (3) characteristic sharp aragonite increases at each aragonite cycle boundary, and (4) generally good correlation between the aragonite variations and the established Pliocene paleoceanographic record (i.e., carbonate preservation record in the equatorial Pacific Ocean), the aragonite variations seem to be much more finely attuned to the global ocean atmosphere carbon system than to only the simple flooding and exposure of shallow carbonate banks. The Quaternary aragonite cycles and supercycles, as well as the Pliocene aragonite variations, are interpreted to represent changes in climatically induced carbonate preservation/dissolution at intermediate water depths of the aragonite bank input, the latter modulated by cyclic bank flooding.

The aragonite record in periplatform ooze will thus become highly valuable in linking the carbonate system between ocean and atmosphere, especially since its primary signal is still preserved back to the early Pliocene. This record will become more global in the next few years through studies in progress on periplatform sequences in the Maldives (Indian Ocean, ODP Leg 115), and possibly sequences in Northeast Australia (future ODP drilling proposed on the Queensland Plateau).

ACKNOWLEDGMENTS

This research was supported in part by a grant from USSAC-JOI to Droxler and Schlager and by funds to Schlager from the Industrial Associates of the Comparative Sedimentology Laboratory of the University of Miami. We thank personnel of the ODP Core Repository of Lamont-Doherty Geological Observatory, particularly Robert Hayman for help during the core sampling, and Tony Barros, Andy Fischer, Terry Hood, Chris Johnson, and Nancy Whittipenn, all at the Rosenstiel School of Marine and Atmospheric Science, University of Miami, for help during sample processing and analyses. We are particularly grateful to Douglas Williams, who made available the Stable Isotope Laboratory at the University of South Carolina, and to Geoffrey A. Haddad, who provided unpublished data from his master's thesis. We had helpful discussions with Wolfgang Schlager, Douglas Williams, and Robert Thunell during the data interpretation. Larry C. Peterson, James A. Austin, Jr., Amanda A. Palmer, and an anonymous reviewer thoroughly reviewed an early draft of the manuscript and made many useful suggestions. Julie Earle at the University of South Carolina typed the first draft. Arista Walters of Rice University typed the final version, and Chingju Liu, also at Rice, drew the final figures on very short notice.

REFERENCES

- Adelseck, C. G., Jr., 1977. Recent and late Pleistocene sediments from the Eastern Equatorial Pacific Ocean: Sedimentation and Dissolution [Ph.D. dissert.]. Univ. California, San Diego.
- Austin, J. A., Jr., Schlager, W., et al., 1986. *Proc. ODP, Init. Repts.*, 101: College Station, TX (Ocean Drilling Program).
- Berggren, W. A., Kent, D. V., and Van Couvering, J. A., 1985. Neogene geochronology and chronostratigraphy. In Snelling, M. H. (Ed.), *Geochronology and the Geologic Time Scale*: Geol. Soc. London Mem., 10:111-160.
- Birch, G. F., 1979. In progress reports of the year 1978. *Cape Town, Univ. Dept. Geol., Mar. Geol. Program, Tech. Rep.*, 11:122-126.
- Boardman, M. R., and Neumann, A. C., 1984. Sources of periplatform carbonates: Northwest Providence Channel, Bahamas. *J. Sediment. Petrol.*, 54:1110-1112.
- _____, 1985. Sources of periplatform carbonates: Northwest Providence Channel, Bahamas—Reply. *J. Sediment. Petrol.*, 55:929-931.
- _____, 1986. Reply on "Banktop responses to Quaternary fluctuations in sea level recorded in periplatform sediments." *Geology*, 14: 1040-1041.
- Boardman, M. R., Neumann, A. C., Baker, P. A., Dulin, L. A., Kenter, R. J., Hunter, G. E., and Kiefer, K. B., 1986. Banktop responses to Quaternary fluctuations in sea level recorded in periplatform sediments. *Geology*, 14:28-31.
- Crevello, P. D., and Schlager, W., 1980. Carbonate debris sheets and turbidites, Exuma Sound, Bahamas. *J. Sediment. Petrol.*, 50:1121-1148.
- Crowley, T. J., 1985. Late Quaternary carbonate changes in the North Atlantic and Atlantic/Pacific comparisons. In Sundquist, E. T., and

- Broecker, W. S. (Eds.), *The Carbon Cycle and Atmospheric CO₂: Natural Variations, Archean to Present*: Geophys. Monogr., 32:271-284.
- Droxler, A. W., 1984. Late Quaternary glacial cycles in the Bahamian deep basins and in the adjacent Atlantic Ocean [Ph.D. dissert.] Univ. Miami, Coral Gables.
- , 1986a. Worldwide occurrence of periplatform aragonite cycles: a record of climatically induced fluctuations of carbonate saturation in intermediate water masses. 12th Int. Sedimentol. Congr., Canberra, Australia, *Abstracts*, 86. (Abstract)
- , 1986b. Comment on "Banktop responses to Quaternary fluctuations in sea level recorded in periplatform sediments." *Geology*, 14:1039-1040.
- Droxler, A. W., and Schlager, W., 1985a. Glacial versus interglacial sedimentation rates and turbidite frequency in the Bahamas. *Geology*, 13:799-802.
- , 1985b. Sources of periplatform carbonates: Northwest Providence Channel, Bahamas—Discussion. *J. Sediment. Petrol.*, 55:928-929.
- Droxler, A. W., Schlager, W., and Whallon, C. C., 1983. Quaternary aragonite cycles and oxygen-isotope record in Bahamian carbonate ooze. *Geology*, 11:235-239.
- Ericson, D. B., and Wollin, G., 1968. Pleistocene climate and chronology in deep-sea sediments. *Science*, 162:1227-1234.
- Haddad, G. A., 1986. A study of carbonate dissolution, stable isotope chemistry and minor element composition of pteropods and forams deposited in the Northwest Providence Channel, Bahamas, during the past 500,000 years [M.S. thesis]. Duke Univ., Durham.
- Haq, B. U., Hardenbol, J., and Vail, P. R., 1987. Chronology of fluctuating sea levels since the Triassic. *Science*, 235:1156-1167.
- Harland, W. B., Cox, A. V., Llewellyn, P. G., Pickton, C.A.G., Smith, A. G., and Walters, R., 1982. *A Geologic Time Scale*: Cambridge (Cambridge Univ. Press).
- Hays, J. D., Saito, T., Opdyke, N. D., and Burckle, L. H., 1969. Pliocene-Pleistocene sediments of the equatorial Pacific: their paleomagnetic, biostratigraphic, and climatic record. *Geol. Soc. Am. Bull.*, 80:1481-1514.
- Hodell, D. A., and Kennett, J. P., 1986. Late Miocene-early Pliocene stratigraphy and paleoceanography of the South Atlantic and southwest Pacific oceans: a synthesis. *Paleoceanography*, 1:285-311.
- Keifer, K. B., 1983. Quaternary climatic cycles recorded in the isotope record of periplatform pelagic deposition: Northwest Providence Channel, Bahamas [M.S. thesis]. Duke Univ., Durham.
- Kier, J. S., and Pilkey, O. H., 1971. The influence of sea level changes on sediment carbonate mineralogy, Tongue of the Ocean, Bahamas. *Mar. Geol.*, 11:189-200.
- King, P. B., 1969. Tectonic Map of North America: U.S. Geol. Surv.
- Milliman, J. D., 1974. *Marine Carbonates*: New York (Springer-Verlag).
- Müller, G., and Gastner, M., 1971. The "Karbonat-Bombe," a simple device for the determination of the carbonate content in sediments, soils and other materials. *N. Jahrb. Mineral. Monatsh.*, 10:466-469.
- Peterson, L. C., and Prell, W. L., 1985. Carbonate preservation and rates of climatic change: an 800 Kyr record from the Indian Ocean. In Sundquist, E. T., and Broecker, W. S. (Eds.), *The Carbon Cycle and Atmospheric CO₂: Natural Variations, Archean to Present*: Geophys. Monogr., 32:251-269.
- Prell, W. L., 1982. Oxygen and carbon isotope stratigraphy for the Quaternary of Hole 502B: evidence for two modes of isotopic variability. In Prell, W. L., and Gardner, J. F., et al., *Init. Repts. DSDP*, 68: Washington (U.S. Govt. Printing Office), 455-464.
- Saito, T., Burckle, L. H., and Hays, J. D., 1975. Late Miocene to Pleistocene biostratigraphy of equatorial Pacific sediments. In Saito, T., and Burckle, L. H. (Eds.), *Late Neogene Epoch Boundaries*: New York (Micropaleontol. Press), 226-244.
- Schlager, W., and James, N. P., 1978. Low-magnesian calcite limestones forming at the deep-sea floor, Tongue of the Ocean, Bahamas. *Sedimentology*, 15:675-702.
- Shackleton, N. J., Backman, J., Zimmerman, H., Kent, D. V., Hal, M. A., and Scientific Party of DSDP Leg 81, 1984. Oxygen isotope calibration of the onset of ice-raftering and history of glaciation in the North Atlantic region. *Nature*, 307, 5952:620-623.
- Shackleton, N. J., and Opdyke, N. D., 1976. Oxygen-isotope and paleomagnetic stratigraphy of Pacific core V28-239, late Pliocene to latest Pleistocene. In Cline, R. M., and Hays, J. D. (Eds.), *Investigations of Late Quaternary Paleoceanography and Paleoclimatology*: Geol. Soc. Am. Mem., 145:449-464.
- Slowey, N. C., 1985. Fine scale acoustic stratigraphy of Northwest Providence Channel, Bahamas [M.S. thesis]. Univ. North Carolina, Chapel Hill.
- Supko, P. R., 1963. A quantitative X-ray diffraction method for the mineralogical analysis of carbonate sediments from Tongue of the Ocean [M.S. thesis]. Univ. Miami, Coral Gables.
- Thierstein, H. R., Geitzenauer, K. R., Molfino, B., and Shackleton, N. J., 1977. Global synchronicity of Late Quaternary coccolith datum levels: validation by oxygen isotopes. *Geology*, 5:400-405.
- Van Donk, J., 1976. O¹⁸ record of the Atlantic Ocean for the entire Pleistocene Epoch. In Cline, R. M., and Hays, J. D. (Eds.), *Investigations of Late Quaternary Paleoceanography and Paleoclimatology*: Geol. Soc. Am. Mem., 145:147-163.
- Vincent, E., 1985. Distribution stratigraphique de la teneur en carbonate dans les sédiments néogènes et quaternaires de l'océan Pacifique. *Bull. Soc. Géol. France*, 8, t.1, 6:915-924.

Date of initial receipt: 17 December 1986

Date of acceptance: 6 January 1988

Ms 101B-134

APPENDIX
Oxygen-Isotope Record and Carbonate Mineralogy of the Top Part of Hole 633A
 Using *Globigerinoides sacculifera* and *G. rubra*

Core, section, interval (cm)	Cumulative depth (cm)	Carbonate (%)	Coarse fraction (%)	Carbonate mineralogy				$\delta^{18}\text{O}$ <i>G. sacculifera</i> and <i>G. rubra</i> *
				Aragonite (%)	Calcite (%)	Magnesian calcite (%)	Dolomite (%)	
Core 1 - Section 1								
5-7	5 - 7	93	23	75	13	12	0	-1.69*
15-17	15 - 17	93	18	68	20	12	0	-1.30
25-27	25 - 27	93	19	66	22	13	0	-0.16*
35-37	35 - 37	93	23	57	30	13	0	
45-47	45 - 47	85	20	34	58	8	0	-0.54*
55-57	55 - 57	86	24	36	47	17	0	0.13*
65-67	65 - 67	93	15	59	25	16	0	0.70
75-77	75 - 77	94	21	58	30	12	0	-0.35*
85-87	85 - 87	95	32	61	27	12	0	-0.37*
95-97	95 - 97	91	18	48	39	13	0	-0.04*
105-107	105 - 107	93	19	49	39	13	0	-0.22*
112-114	115 - 117	93	23	53	35	12	0	0.38*
125-127	125 - 127	92	18	49	37	13	0	0.20*
135-137	135 - 137	92	16	46	45	10	0	-0.02*
145-147	145 - 147	92	14	50	42	7	0	0.12*
Section 2								
5-7	155 - 157	91	17	49	47	4	0	-0.45*
15-17	165 - 167	94	24	54	38	8	0	-0.18
25-27	175 - 177	90	19	35	57	11	0	0.17
35-37	185 - 187	88	16	44	45	10	0	-0.91
45-47	195 - 197	93	15	53	37	10	0	-0.91
55-57	205 - 207	96	17	62	28	11	0	0.08
65-67	215 - 217	96	22	59	30	12	0	-0.59
75-77	225 - 227	94	18	55	33	10	0	0.29
85-87	235 - 237	95	16	55	35	13	0	0.03
95-97	245 - 247	95	22	59	29	11	0	0.53
105-107	255 - 257	95	25	70	19	9	0	0.09
117-118	265 - 268	96	18	72	19	9	0	-0.16
125-127	275 - 277	96	18	71	20	9	0	-0.20
135-137	285 - 287	96	19	66	26	8	0	-0.18
145-147	295 - 297	95	21	64	25	11	0	-0.03
Section 3								
5-7	305 - 307	94	18	62	32	6	0	
13-15	313 - 315	94	17	66	26	7	0	-0.34
35-37	335 - 337	94	18	65	30	5	0	-1.03
45-47	345 - 347	91	25	38	60	2	0	0.28
55-57	355 - 357	91	20	51	47	2	0	
65-67	365 - 367	91	18	50	41	8	0	0.10
75-77	375 - 377	92	28	49	45	6	0	-0.28
85-87	385 - 387	91	16	54	38	8	0	
95-97	395 - 397	91	24	50	40	10	0	0.27*
105-107	405 - 407	91	22	49	43	8	0	0.30*
117-119	417 - 419	4	16	54	41	5	0	-0.16*
125-127	425 - 427	93	16	46	47	6	0	-0.67*
135-137	435 - 437	93	16	54	40	6	0	-1.60*
145-147	445 - 447	91	18	44	49	6	0	-1.40*
Section 4								
5-7	455 - 457	91	17	49	43	8	0	
15-17	465 - 467	91	18	43	50	7	0	-0.46
25-27	475 - 477	95	26	55	39	6	0	-0.33
35-37	485 - 487	95	24	65	26	9	0	-0.93
45-47	495 - 497	95	21	60	34	5	0	-1.74
55-57	505 - 507	94	18	56	36	8	0	-0.55
65-67	515 - 517	93	14	49	49	2	0	-0.44
75-77	525 - 527	94	15	59	39	2	0	-0.65*
85-87	535 - 537	95	13	58	37	4	0	-1.11
95-97	545 - 547	92	12	43	52	5	0	-1.91*
105-107	555 - 557	92	12	58	39	3	0	
117-119	567 - 569	92	18	54	45	2	0	0.63
125-127	575 - 577	94	15	54	46	0	0	-0.91
135-137	585 - 587	94	11	48	52	0	0	-1.47*
145-147	595 - 597	92	12	22	78	0	0	-0.22*

Core, section, interval (cm)	Cumulative depth (cm)	Carbonate (%)	Coarse fraction (%)	Carbonate mineralogy				$\delta^{18}\text{O}$ <i>G. sacculifera</i> and <i>G. rubra</i> *
				Aragonite (%)	Calcite (%)	Magnesian calcite (%)	Dolomite (%)	
Section 5								
5-7	605 - 607	90	24	25	74	0	1	
15-17	615 - 617	91	29	21	79	0	0	
25-27	625 - 627	94	6	45	55	0	0	
45-47	645 - 647	92	17	30	70	0	0	
55-57	655 - 657	91	16	37	63	0	0	-1.33*
65-67	665 - 667	91	11	29	71	0	0	-1.04*
75-77	675 - 677	94	11	34	66	0	0	-1.62*
85-87	685 - 687	95	10	36	64	0	0	-0.98*
95-97	695 - 697	95	9	37	63	0	0	-1.17*
105-107	705 - 707	91	15	32	68	0	0	0.52
117-119	717 - 719	94	10	39	61	0	0	
125-127	725 - 727	93	12	36	64	0	0	0.41
135-137	735 - 737	94	9	38	62	0	0	-0.82
Section 6								
5-7	755 - 757	96	13	37	63	0	0	-0.54
15-17	765 - 767	94	14	27	73	0	0	-0.39
25-27	775 - 777	93	14	33	67	0	0	-0.19
35-37	785 - 787	94	11	44	56	0	0	-0.74
45-47	795 - 797	95	14	57	43	0	0	-0.95
55-57	805 - 807	95	14	63	37	0	0	-0.73
65-67	815 - 817	94	10	71	29	0	0	-0.84
75-77	825 - 827	95	28	11	89	0	0	-0.46
85-87	835 - 837	91	18	5	95	0	0	0.27
95-97	845 - 847	87	10	8	92	0	0	0.66
C/C								
5-7	855 - 857	91	14	22	78	0	1	0.01
15-17	865 - 867	91	15	41	59	0	0	-0.85
Core 2 - Section 1								
5-7	875 - 877	92	12	61	39	0	0	-0.41
15-17	885 - 887	94	9	70	30	0	0	0.84
25-27	895 - 897	94	8	56	44	0	0	-1.98
35-37	905 - 907	94	12	40	60	0	0	0.70
45-47	915 - 917	92	12	33	67	0	0	0.36
55-57	925 - 927	87	14	32	68	0	0	0.98
65-67	935 - 937	87		42	58	0	0	1.18
75-77	945 - 947	92	10	36	62	0	2	0.74
85-87	955 - 957	88	12	29	71	0	0	0.42
95-97	965 - 967	91	9	57	43	0	0	1.43
105-107	975 - 977	93	9	27	73	0	0	0.54
115-117	985 - 987	91	10	43	57	0	0	0.30
125-127	995 - 997	89	12	33	67	0	0	0.04
135-137	1005 - 1007	94	9	49	51	0	0	0.18
145-147	1015 - 1017	94	11	62	38	0	0	-0.17
Section 2								
5-7	1025 - 1027	83	10	47	49	0	3	-0.50
15-17	1035 - 1037	82	7	36	62	0	2	0.88
25-27	1045 - 1047	98	10	36	64	0	0	1.00
35-37	1055 - 1057	96	9	32	68	0	0	1.08
45-47	1065 - 1067	98	9	13	87	0	0	1.13
52-54	1072 - 1074	987	10	12	88	0	0	1.25
65-67	1085 - 1087	92	8	5	95	0	0	1.42
75-77	1095 - 1097	98	11	29	71	0	0	1.09
85-87	1105 - 1107	94	10	26	74	0	0	0.84
95-97	1115 - 1117	91	10	20	79	0	1	1.00
105-107	1125 - 1127	92	10	27	72	0	1	0.81
115-117	1135 - 1137	91	11	25	75	0	0	0.73
125-127	1145 - 1147	94	12	50	50	0	0	0.92
135-137	1155 - 1157		12					0.85
145-147	1165 - 1167	95	15	45	55	0	0	-0.11
Section 3								
5-7	1175 - 1177	95	13	51	49	0	0	-1.20
15-17	1185 - 1187	89	13	47	53	0	0	0.21
23-25	1193 - 1195	97	12	53	47	0	0	
35-37	1205 - 1207	97	19	67	33	0	0	
45-47	1215 - 1217	89	17	43	57	0	0	
53-55	1223 - 1225	94	17	56	44	0	0	

ARAGONITE CONTENT AND OXYGEN-ISOTOPE RECORD

Core, section, interval (cm)	Cumulative depth (cm)	Carbonate (%)	Coarse fraction (%)	Carbonate mineralogy				$\delta^{18}\text{O}$ <i>G. sacculifera</i> and <i>G. rubra</i> *
				Aragonite (%)	Calcite (%)	Magnesian calcite (%)	Dolomite (%)	
65-67	1235 - 1237	94	21	43	57	0	0	
75-77	1245 - 1247	94	17	56	43	1	0	
85-87	1255 - 1257	94	17	62	33	5	0	
95-97	1265 - 1267	97	15	69	27	4	0	-0.75
105-107	1275 - 1277	96	18	53	46	1	0	0.49
115-117	1285 - 1287	92	24	67	30	3	0	0.68
125-127	1295 - 1297	96	23	56	42	2	0	0.18
135-137	1305 - 1307	96	19	62	35	3	0	-1.00
145-147	1315 - 1317	95	19	68	31	1	0	-0.14
Section 4								
5-7	1325 - 1327	93	16	69	28	0	0	-0.46
15-17	1335 - 1337	94	15	70	25	5	0	0.54
25-27	1345 - 1347		13					0.06
35-37	1355 - 1357	91	16	70	25	5	0	-0.28
45-47	1365 - 1367	89	11	71	27	2	0	0.03
55-57	1375 - 1377	96	12	61	39	0	0	0.45
69-71	1389 - 1391	93	17	30	70	0	0	0.92
75-77	1395 - 1397	92	17	33	67	0	0	0.26
85-87	1405 - 1407	89	13	60	35	0	0	0.49
95-97	1415 - 1417	93	13	21	79	0	0	0.49
105-107	1425 - 1427	94	18	51	49	0	0	0.43
115-117	1435 - 1437	77	18	25	75	0	0	1.03
125-127	1445 - 1447	92	16	56	44	0	0	1.21
135-137	1455 - 1457	87	14	40	60	0	0	0.74
145-147	1465 - 1467	87	17	58	42	0	0	
Section 5								
5-7	1475 - 1477	91	19	49	51	0	0	0.45
15-17	1485 - 1487	93	18	44	56	0	0	-0.37
25-27	1495 - 1497	91	17	52	48	0	0	-0.64
35-37	1505 - 1507	94	15	58	42	0	0	-0.07
45-47	1515 - 1517	88	11	65	33	0	2	-0.69
53-55	1523 - 1525	95	13	49	51	0	0	-0.38
65-67	1535 - 1537	94	19	37	63	0	0	0.43
75-77	1545 - 1547	92	18	34	66	0	0	-0.18
85-87	1555 - 1557	95	10	38	62	0	0	-0.28
95-97	1565 - 1567	96	14	50	50	0	0	0.11
105-107	1575 - 1577	92	13	39	61	0	0	0.12
115-117	1585 - 1587	94	15	37	63	0	0	0.40
125-127	1595 - 1597	95	14	32	68	0	0	
135-137	1605 - 1607	95	17	31	69	0	0	
Section 6								
5-7	1625 - 1627	91	16	34	66	0	0	0.80
15-17	1635 - 1637	93	17	43	57	0	0	1.02
25-27	1645 - 1647	94	11	38	62	0	0	1.11
35-37	1655 - 1657	95	10	38	62	0	0	0.65
45-47	1665 - 1667	96	12	45	55	0	0	0.62
53-57	1673 - 1675	98	10	51	49	0	0	-0.03
65-67	1685 - 1687	97	10	49	51	0	0	0.78
75-77	1695 - 1697	96	8	50	50	0	0	0.34
85-87	1705 - 1707	97	10	43	57	0	0	
95-97	1715 - 1717	96	28	26	74	0	0	-0.11
105-107	1725 - 1727	96	10	22	78	0	0	1.18
121-123	1741 - 1743	93	27	39	61	0	0	1.89
Core 3 - Section 1								
4-5	1764 - 1766	96	19	40	60	0	0	0.53
16-17	1776 - 1777	96	18	41	59	0	0	0.40
24-25	1784 - 1785	96	16	42	58	0	0	-0.13
34-35	1794 - 1795	94	18	53	47	0	0	0.02
44-45	1804 - 1805	95	20	51	44	5	0	
54-55	1814 - 1815	96	17	56	40	4	0	-0.08
64-65	1824 - 1825	95	14	57	35	8	0	0.06
73-74	1833 - 1834	94	26	59	36	5	0	-0.17
84-85	1844 - 1845	96	16	60	35	5	0	-0.25
94-95	1854 - 1855	96	15	65	32	2	0	0.57
104-105	1864 - 1865	97	13	62	31	7	0	-0.34
114-115	1874 - 1875	95	23	59	33	8	0	-0.36
124-125	1884 - 1885	95	22	62	35	3	0	0.23

Core, section, interval (cm)	Cumulative depth (cm)	Carbonate (%)	Coarse fraction (%)	Carbonate mineralogy				$\delta^{18}\text{O}$ <i>G. sacculifera</i> and <i>G. rubra</i> *
				Aragonite (%)	Calcite (%)	Magnesian calcite (%)	Dolomite (%)	
137-138	1897 - 1898	95	15	63	31	7	0	0.04
143-145	1903 - 1905	95	11	62	24	13	0	
Section 2								
4-5	1914 - 1915	94	16	61	35	4	0	-0.27
14-15	1924 - 1925	94	16	72	21	7	0	-0.63
24-25	1934 - 1935	94	15	72	24	3	0	-0.69
34-35	1944 - 1945	95	16	79	14	7	0	-0.63
44-45	1954 - 1955	94	14	77	18	5	0	
53-54	1963 - 1964	94	13	81	14	5	0	
64-65	1974 - 1975	95	15	76	21	3	0	
74-75	1984 - 1985	95	18	71	24	5	0	-1.48
84-85	1994 - 1995	94	18	62	38	0	0	-1.27
104-105	2014 - 2015	88	15	8	92	0	0	-1.21
114-115	2024 - 2025	86	12	19	79	0	2	-0.42
124-125	2034 - 2035	88	18	17	82	0	1	0.53
134-135	2044 - 2045	90	11	34	66	0	0	-1.16
144-145	2054 - 2055	93	18	35	65	0	0	-0.38
Section 3								
4-5	2064 - 2065	95	18	39	61	0	0	-0.76
14-15	2074 - 2075	95	19	42	58	0	0	-0.72
24-25	2084 - 2085	94	9	67	33	0	0	-1.54
43-44	2103 - 2104	91	13	33	67	0	0	-0.33
53-54	2113 - 2114	92	17	38	62	0	0	-1.45
64-65	2123 - 2124	94	21	30	70	0	0	-1.08
74-75	2133 - 2134		21					-0.78
84-85	2144 - 2145	96	19	37	63	0	0	-0.48
94-95	2154 - 2155	94	17	37	63	0	0	0.63
104-105	2164 - 2165	94	20	43	57	0	0	0.02
114-115	2174 - 2175	94	22	36	64	0	0	0.46
124-125	2184 - 2185	96	18	42	58	0	0	0.58
134-135	2194 - 2195	97	18	21	79	0	0	
144-145	2204 - 2205	96	15	35	65	0	0	0.63
Section 4								
5-7	2215 - 2217	93	8	32	68	0	0	0.55
15-17	2225 - 2227	93	10	46	54	0	0	-0.85
25-27	2235 - 2237	92	11	37	63	0	0	-1.01
35-37	2245 - 2247	91	10	35	65	0	0	-1.05
45-47	2255 - 2257	96	9	37	63	0	0	-1.82
55-57	2265 - 2267	96	10	39	61	0	0	-0.55
65-67	2275 - 2277	96	10	34	66	0	0	-0.53
75-77	2285 - 2287	92	11	41	59	0	0	-0.88
85-87	2295 - 2297	92	12	48	52	0	0	-0.61
95-97	2305 - 2307	91	15	42	58	0	0	-0.06
105-107	2315 - 2317	96	25	45	55	0	0	0.70
115-117	2325 - 2327	96	17	42	58	0	0	0.81
125-127	2335 - 2337	96	15	43	57	0	0	
135-137	2345 - 2347	94	16	46	54	0	0	
Section 5								
3-5	2363 - 2365	98	13	59	41	0	0	-0.11
10-12	2370 - 2372	99	15	60	40	0	0	-0.03
18-20	2378 - 2380	96	14	60	40	0	0	0.11
35-37	2395 - 2397	93	11	15	85	0	0	0.50
45-47	2405 - 2407	93	10	22	78	0	0	0.51
55-57	2415 - 2417	93	13	26	74	0	0	0.62
65-67	2425 - 2427	97	9	44	56	0	0	0.07
75-77	2435 - 2437	97	11	35	65	0	0	-0.17
87-89	2447 - 2449	93	11	34	66	0	0	-0.10
95-97	2455 - 2457	91	8	33	65	0	2	0.03
105-107	2465 - 2467	93	10	33	67	0	0	0.28
115-117	2475 - 2477	95	19	50	49	0	1	
Section 6								
15-17	2515 - 2517	92	12	42	58	0	0	-0.55
25-27	2525 - 2527	96	14	46	54	0	0	-0.26
34-36	2535 - 2537	97	14	48	52	0	0	-0.31
45-47	2544 - 2546	96	17	56	44	0	0	-0.53
55-57	2555 - 2557	96	17	53	47	0	0	-1.57
69-71	2579 - 2580	97	19	59	41	0	0	
			25	70	30	0	0	-0.94

ARAGONITE CONTENT AND OXYGEN-ISOTOPE RECORD

Core, section, interval (cm)	Cumulative depth (cm)	Carbonate (%)	Coarse fraction (%)	Carbonate mineralogy				$\delta^{18}\text{O}$ <i>G. sacculifera</i> and <i>G. rubra</i> *
				Aragonite (%)	Calcite (%)	Magnesian calcite (%)	Dolomite (%)	
85-87	2595 - 2597	97	13	65	35	0	0	-1.49
95-97	2605 - 2607	92	10	46	54	0	0	-1.51
105-107	2615 - 2617	91	12	36	64	0	0	-0.20
115-117	2625 - 2627	92	11	24	76	0	0	-1.22
125-127	2635 - 2637	92	13	31	68	0	1	-0.56
135-137	2645 - 2647	92	13	28	72	0	0	0.07
145-147	2655 - 2657	92	11	44	56	0	0	0.61
Core 4 - Section 1								
5-7	2717 - 2719	96	29	53	47	0	0	-0.37
15-17	2727 - 2729	95	19	59	41	0	0	0.08
55-57	2767 - 2769	92	10	41	59	0	0	0.02
65-67	2777 - 2779	92	11	32	68	0	0	-0.61
75-77	2787 - 2789	91	13	40	60	0	0	-0.35
85-87	2797 - 2799	90	16	49	51	0	0	1.01
95-97	2807 - 2809	92	18	48	52	0	0	0.14
125-127	2837 - 2839	90	16	46	54	0	0	0.12
135-137	2847 - 2849	93	15	53	47	0	0	-0.06
145-147	2857 - 2859	95	14	54	46	0	0	-1.04
Section 2								
5-7	2867 - 2869	97	14	57	43	0	0	-2.68
15-17	2877 - 2879	95	12	66	34	0	0	-0.68
25-27	2887 - 2889	97	16	68	32	0	0	0.2
35-37	2897 - 2899	97	6	60	40	0	0	-0.73
65-67	2927 - 2929	95	42	32	68	0	0	0.26
95-97	2957 - 2959	95	10	54	46	0	0	-0.98
105-107	2967 - 2969	96	20	56	44	0	0	-0.66
115-117	2977 - 2979	97	16	64	36	0	0	
125-127	2987 - 2989	94	15	68	32	0	0	-0.46
135-137	2997 - 2999	90	8	66	34	0	0	-1.17
145-147	3007 - 3009	94	7	68	32	0	0	
Section 3								
5-7	3017 - 3019	95	7	50	50	0	0	-1.22
15-17	3027 - 3029	94	51	28	72	0	0	-1.62
51-53	3063 - 3065	95	19	38	62	0	0	-0.21
57-59	3009 - 3071	96	23	40	60	0	0	-1.06
65-67	3077 - 3079	96	8	54	46	0	0	-1.51
85-87	3097 - 3099	95	15	47	53	0	0	-0.33
105-107	3117 - 3119	97	12	54	46	0	0	-0.52
115-117	3127 - 3129	95	19	56	44	0	0	-0.76
125-127	3137 - 3139	96	9	53	47	0	0	-1.18
135-137	3147 - 3149	96	13	54	46	0	0	-0.71
145-147	3157 - 3159	96	13	64	36	0	0	-0.87
Section 4								
5-7	3167 - 3169	80	9	48	52	0	0	-1.45
15-17	3177 - 3179	93	40	15	85	0	0	-1.31
25-27	3187 - 3189	90	17	24	76	0	0	0.04
35-37	3197 - 3199	96	13	49	51	0	0	-1.44
45-47	3207 - 3209	97	11	55	45	0	0	
55-57	3217 - 3219	97	10	61	39	0	0	-0.69
65-67	3227 - 3229	96	14	59	41	0	0	-0.86
75-77	3237 - 3239		17		100	0	0	
85-87	3247 - 3249	88	12	63	37	0	0	-1.21
95-97	3257 - 3259	95	8	57	43	0	0	
105-107	3267 - 3269	95	14	39	61	0	0	-0.24
115-117	3277 - 3279	93	15	8	92	0	0	-0.07
125-127	3287 - 3289	87	17	31	69	0	0	0.06
135-137	3297 - 3299	96	14	51	49	0	0	-0.16
Section 5								
5-7	3317 - 3319	94	12	27	73	0	0	-1.03
15-17	3327 - 3329	94	11	40	60	0	0	-0.92
23-25	3337 - 3339	93	13	42	58	0	0	-2.24
35-37	3347 - 3349	97	12	49	51	0	0	-1.79
45-47	3357 - 3359	86	9	21	79	0	0	-0.03
53-55	3365 - 3367	93	12	13	87	0	0	-0.95
65-67	3377 - 3379	92	27	33	67	0	0	-0.07
74-76	3386 - 3388	87	9	23	77	0	0	-0.85
85-87	3397 - 3399	98	17	60	40	0	0	-0.60

Core, section, interval (cm)	Cumulative depth (cm)	Carbonate (%)	Coarse fraction (%)	Carbonate mineralogy				$\delta^{18}\text{O}$ <i>G. sacculifera</i> and <i>G. rubra</i> *
				Aragonite (%)	Calcite (%)	Magnesian calcite (%)	Dolomite (%)	
95-97	3407 - 3409	94	11		100	0	0	-1.48
105-107	3417 - 3419	94	21	61	39	0	0	-1.69
114-116	3426 - 3428	94	20	40	60	0	0	-0.77
125-127	3437 - 3439	94	16	44	56	0	0	-0.03
135-137	3447 - 3449	97	11	61	39	0	0	-0.15
145-147	3457 - 3459	97	7	72	28	0	0	-0.13
Section 6								
5-7	3467 - 3469	97	4	79	21	0	0	-1.61
15-17	3477 - 3479	80	5	71	29	0	0	-0.73
25-27	3487 - 3489	95	14	65	35	0	0	-0.36
35-37	3497 - 3499	86	9	50	50	0	0	-0.45
45-47	3507 - 3509	94	69	36	64	0	0	-1.48
55-57	3517 - 3519	92	18	35	65	0	0	-1.48
69-71	3531 - 3533	97	11	56	44	0	0	-0.46
99-101	3561 - 3563	95	35	52	48	0	0	
121-123	3585 - 3587	95	10	65	35	0	0	-1.48
135-137	3597 - 3599	80	11	16	84	0	0	0.13
145-147	3607 - 3609	85	16	10	90	0	0	-0.52
Section 7								
5-7	3617 - 3619		16	7	93	0	0	
Core 5 - Section 1								
15-17	3640 - 3642	94	26	34	66	0	0	-0.73
35-37	3660 - 3662	92	13	41	59	0	0	-0.87
45-47	3670 - 3672	86	47	16	84	0	0	0.46
55-57	3680 - 3682	89	16	8	92	0	0	0.75
65-67	3690 - 3692	93	12	20	80	0	0	-1.40
75-77	3700 - 3702	97	24	36	64	0	0	-0.49
85-87	3710 - 3712	94	13	28	72	0	0	-0.45
95-97	3720 - 3722	95	16	1	99	0	0	-0.22
105-107	3730 - 3732	95	17	0	100	0	0	-0.44
115-117	3740 - 3742	96	14	0	100	0	0	-1.26
125-127	3750 - 3752	95	21	0	100	0	0	-0.74
135-137	3760 - 3762	97	11	6	94	0	0	0.51
145-147	3770 - 3772	93	8	28	72	0	0	-0.09
Section 2								
5-7	3780 - 3782	91	18	16	84	0	0	-0.35
15-17	3790 - 3792	98	8	51	49	0	0	-0.51
25-27	3800 - 3802	97	8	51	49	0	0	0.17
35-37	3810 - 3812	98	14	28	72	0	0	0.28
45-47	3820 - 3822	96	42	14	86	0	0	
55-57	3830 - 3832	95	17	14	86	0	0	-0.24
65-67	3840 - 3842	97	11		100	0	0	-1.51
75-77	3850 - 3852	94	10	0	100	0	0	0.14
85-87	3860 - 3862	90	15		100	0	0	
95-97	3870 - 3872	92	19		100	0	0	-0.34
105-107	3880 - 3882	98	28	0	100	0	0	
115-117	3890 - 3892	95	28	13	87	0	0	-0.00
125-127	3900 - 3902	94	37	0	100	0	0	-0.93
135-137	3910 - 3912	91	18	0	100	0	0	
145-147	3920 - 3922	97	20	0	100	0	0	-0.65
Section 3								
5-7	3930 - 3932	97	13	0	100	0	0	-0.24
15-17	3940 - 3942	97	17	0	100	0	0	
23-25	3948 - 3950	97	17	0	100	0	0	-0.17
35-37	3960 - 3962	97	28	0	100	0	0	-0.57
45-47	3970 - 3972	97	38	0	100	0	0	-0.49
55-57	3980 - 3982	97	36	0	100	0	0	-0.29
65-67	3990 - 3992	99	32	0	100	0	0	-0.48
75-77	4000 - 4002	94	43	0	100	0	0	0.89
85-87	4010 - 4012	94	42	0	100	0	0	0.46
95-97	4020 - 4022	95	36	15	85	0	0	0.24
105-107	4030 - 4032	100	51	18	82	0	0	0.17
115-117	4040 - 4042	99	43	30	70	0	0	-0.44
125-127	4050 - 4052	100	43	21	79	0	0	-0.68
135-137	4060 - 4062	98	38	29	71	0	0	-0.32
145-147	4070 - 4072	99	57	30	70	0	0	-0.28

ARAGONITE CONTENT AND OXYGEN-ISOTOPE RECORD

Core, section, interval (cm)	Cumulative depth (cm)	Carbonate (%)	Coarse fraction (%)	Carbonate mineralogy				$\delta^{18}\text{O}$ <i>G. sacculifera</i> and <i>G. rubra</i> *
				Aragonite (%)	Calcite (%)	Magnesian calcite (%)	Dolomite (%)	
Section 4								
5-7	4080 - 4082	96	30	48	52	0	0	-1.30
15-17	4090 - 4092	93	20	49	51	0	0	-0.02
25-27	4100 - 4102	96	24	35	65	0	0	-1.07
35-37	4110 - 4112	92	15	47	53	0	0	-0.99
45-47	4120 - 4122	95	18	38	62	0	0	-0.70
55-57	4130 - 4132	96	41	25	75	0	0	-1.70
65-67	4140 - 4142	93	52	14	86	0	0	-0.66
75-77	4150 - 4152	93	53	0	100	0	0	-0.56
95-97	4170 - 4172	94	49	0	100	0	0	-0.30
105-107	4180 - 4182	89	27	0	100	0	0	0.13
115-117	4190 - 4192	90	37	0	100	0	0	-0.38
125-127	4200 - 4202	90	23	0	100	0	0	-0.68
135-137	4210 - 4212	84	26	0	100	0	0	-0.27
145-147	4220 - 4222	92	28	0	100	0	0	-0.27
Section 5								
4-5	4229 - 4230	97	15	0	100	0	0	0.33
14-15	4239 - 4240	98	19	0	100	0	0	0.15
24-25	4249 - 4250	96	15	0	100	0	0	-0.05
34-35	4259 - 4260	96	12	0	100	0	0	0.22
43-44	4268 - 4269	97	15	7	93	0	0	-0.07
53-54	4279 - 4280	94	16	0	100	0	0	0.02
64-65	4289 - 4290	93	14	0	100	0	0	
74-75	4299 - 4300	95	14	1	99	0	0	-0.42
84-85	4309 - 4310	98	12	0	100	0	0	
93-94	4318 - 4319	98	12	0	100	0	0	
104-105	4329 - 4330	93	23	0	100	0	0	0.51
115-116	4340 - 4341	91	15	0	100	0	0	-0.29
124-125	4349 - 4350	90	18	0	100	0	0	0.24
134-135	4359 - 4360	93	18	0	100	0	0	
Section 6								
14-15	4389 - 4390	96	13	24	70	0	6	
24-25	4399 - 4400	96	18	32	51	0	17	0.20
34-35	4409 - 4410	97	10	0	68	0	32	-0.16
44-45	4419 - 4420	97	10	0	78	0	22	0.20
54-56	4429 - 4430	97	14	27	60	0	13	
64-65	4439 - 4440	97	10	18	66	0	16	-0.19
74-75	4449 - 4450	98	14	18	67	0	15	-1.07
84-85	4459 - 4460	97	11	31	57	0	12	
94-95	4469 - 4470	97	11	30	60	0	10	-0.08
104-105	4479 - 4480	99	10	22	71	0	7	-0.36
114-115	4489 - 4490	99	9	0	89	0	11	-0.17
124-125	4500 - 4501	99	17	19	78	0	3	-0.38
135-136	4510 - 4511	98	11	19	72	0	9	-0.20
146-147	4521 - 4522	99	7	29	66	0	5	-0.39
Section 7								
4-5	4529 - 4530	95	9	35	58	0	7	-0.18
14-15	4539 - 4540	95	9	34	58	0	7	0.14
24-25	4549 - 4550	97	10	34	60	0	6	0.21
34-35	4559 - 4560	98	8	37	57	0	7	
44-45	4569 - 4570	98	12	41	52	0	7	0.03
Core 6 - Section 1								
4-5	4589 - 4590	96	7	38	57	0	5	
14-15	4599 - 4600	96	9	27	69	0	3	
24-25	4609 - 4610	96	10	36	59	0	4	0.66
34-35	4619 - 4620	98	11	42	53	0	5	-0.18
44-45	4629 - 4630	96	15	42	53	0	6	0.15
53-54	4638 - 4639	96	11	51	43	0	6	-0.12
64-65	4649 - 4650	98	10	54	40	0	6	-0.66
73-74	4658 - 4659	96	13	47	48	0	5	-0.23
83-84	4668 - 4669	98	14	40	56	0	4	-0.83
93-94	4678 - 4679	99	12	31	67	0	2	-0.10
103-104	4688 - 4689	98	10	51	45	0	4	-1.48
113-114	4698 - 4699	99	12	51	46	0	3	
123-124	4708 - 4709	98	10	57	40	0	3	
Section 2								
3-4	4738 - 4740	95	9	57	41	0	1	

Core, section, interval (cm)	Cumulative depth (cm)	Carbonate (%)	Coarse fraction (%)	Carbonate mineralogy				$\delta^{18}\text{O}$ <i>G. sacculifera</i> and <i>G. rubra</i> *
				Aragonite (%)	Calcite (%)	Magnesian calcite (%)	Dolomite (%)	
13-14	4748 - 4749	97	11	57	41	0	2	
24-25	4759 - 4760	97	10	50	49	0	1	
33-34	4768 - 4769	96	14	52	45	0	2	
43-44	4778 - 4779	96	11	53	46	0	3	
53-54	4788 - 4789	97	9	42	55	0	3	
63-64	4798 - 4799	96	9	41	57	0	1	
73-74	4808 - 4809	97	16	38	60	0	2	
84-85	4819 - 4820	99	20	34	63	0	3	
94-95	4829 - 4830	98	11	42	54	0	3	
104-5	4839 - 4840	97	9	35	62	0	3	
115-16	4850 - 4851	97	8	41	57	0	2	
124-25	4859 - 4860	98	8	38	59	0	3	
133-34	4868 - 4869	98	12	32	65	0	3	
144-145	4879 - 4880	98	18	31	65	0	4	
Section 3								
5-7	4890 - 4892	95	46	41	63	0	5	
15-17	4900 - 4902	93	13	34	60	0	6	
23-25	4908 - 4910	93	9	41	54	0	6	
35-32	4920 - 4922	93	12	52	42	0	6	
45-47	4930 - 4932	93	11	43	53	0	5	
55-57	4940 - 4942	93	12	51	44	0	5	
65-67	4950 - 4952	94	11	53	42	0	5	
75-77	4960 - 4962	93	15	59	35	0	6	
85-87	4970 - 4972	93	12	63	32	0	5	
95-97	4980 - 4982	95	10	51	45	0	4	
105-107	4990 - 4996	96	41	42	55	0	3	
115-117	5000 - 5002	97	35	35	61	0	4	
125-127	5010 - 5012	97	56	48	48	0	4	
135-137	5020 - 5022	96	51	51	43	0	6	
145-147	5030 - 5032	95	39	54	41	0	5	
Section 4								
5-7	5040 - 5042	96	56	48	46	0	6	
15-17	5050 - 5052	97	42	54	40	0	7	
25-27	5060 - 5062	98	47	61	33	0	6	
45-47	5080 - 5082	97	52	62	38	0	6	
55-57	5090 - 5092	97	61	58	37	0	5	
65-67	5100 - 5102	96	54	61	34	0	5	
75-77	5110 - 5112	97	57	63	31	0	6	
85-87	5120 - 5122	98	42	69	23	0	7	
95-97	5130 - 5132	97	53	64	31	0	5	
105-107	5140 - 5142	98	56	58	37	0	5	
115-117	5150 - 5152	98	62	61	32	0	7	
125-127	5160 - 5162	98	52	60	33	0	7	
135-137	5170 - 5172	98	52	62	32	0	6	
Section 5								
4-5	5189 - 5190	97	47	65	27	0	8	
54-56	5239 - 5241	96	55	71	22	0	8	
65-67	5250 - 5252	97	56	69	25	0	6	
75-77	5260 - 5262	98	49	68	25	0	7	
85-87	5270 - 5272	97	50	70	24	0	6	
95-97	5880 - 5882	98	55	64	30	0	7	
Section 6								
5-7	5340 - 5346	97	52	68	25	0	6	
25-27	5360 - 5362	97	60	66	28	0	6	
45-47	5380 - 5382	96	49	56	39	0	5	
65-67	5400 - 5402	96	57	64	29	0	7	
85-87	5420 - 5422	96	56	71	33	0	7	
125-127	5460 - 5462	95	57	62	33	0	5	
145-147	5480 - 5482	97	80(1)	51	45	0	4	
c/c								
5-7	5490 - 5492	96	39	58	35	0	7	
25-27	5510 - 5512	95	33	65	29	0	6	
45-47	5530 - 5532	97	54	60	35	0	5	